JOURNAL OF CATALYSIS 131, 545–572 (1991)

# Pyridine Hydrogenation and Piperidine Hydrogenolysis on a Commercial Hydrocracking Catalyst

## I. Reaction and Deactivation Kinetics

G. C. HADJILOIZOU,[1] J. B. BUTT,[2] AND J. S. DRANOFF

*Department of Chemical Engineering, Northwestern University, Evanston, Illinois 60208*

Received March 20, 1991

The vapor phase kinetics of pyridine hydrogenation over a commercial fresh hydrocracking catalyst were studied in a continuous-flow fixed-bed reactor and the feasibility of this reaction as a probe for characterizing the catalyst was examined. Kinetic experiments at total pressures of 13.01 to 13.48 atm, temperatures of 312 to 334°C, and initial pyridine partial pressures of 0.116 to 0.483 atm indicated that pyridine hydrogenation to piperidine was the predominant reaction and that the reaction rate was first order in pyridine. The feasibility of piperidine hydrogenolysis as a probe for characterizing dual-functional catalysts was also examined and the reaction and deactivation kinetics of this system were studied in the above reactor operating at integral conversions. The kinetic studies were conducted at total pressures of 15.86 to 16.14 atm, temperatures ranging from 281 to 321°C, and initial concentrations of piperidine from 4.03 to 11.84 $\times 10^{-3}$ mol/liter. Product distributions revealed that the predominant reactions were only those converting piperidine to other nitrogen-containing compounds. Both the metallic and acidic catalyst functions were active simultaneously in the conversion reactions and both were deactivated under conditions of the experiments. To offset catalyst deactivation effects, the conversion data were extrapolated to zero time on stream. The kinetic parameters were determined using a reaction–deactivation model based on separable kinetics. The reaction rate data were best fit to Langmuir–Hinshelwood type expressions proposing two different catalytic sites for hydrogen and nitrogen compound adsorption. 

## INTRODUCTION

Catalytic hydrocracking is widely used commercially for converting various petroleum cuts to gasoline, jet fuel, diesel fuel, heating and lubricating oils, and LPG. The catalysts used are typically dual-functional, containing both metallic and acidic functions. The balance between these functions can be substantially varied to adjust catalyst selectivity according to the particular application desired. One of the most significant problems encountered in hydrocracking, as in many other catalytic processes, is catalyst deactivation with time on stream. This can occur by coke and metals deposition on the catalyst, by sintering of the metallic function, or by poisoning via highly basic nitrogen compounds. Both catalyst activity and product selectivity can be significantly affected in the deactivation process. Selectivity changes can also be attributed to temperature increases needed to maintain activity. Hence, in predicting reactor performance and product distribution as a function of time on stream, it is essential to understand completely the processes causing activity and selectivity variation. In addition, before developing successful catalyst regeneration techniques a thorough study is needed to understand the mechanisms responsible for changes in activity and selectivity.

An efficient means for characterizing catalysts and also verifying their suitability be-

[1] Present address: Exxon Research and Development Laboratories, P.O. Box 2226, Baton Rouge, LA 70821.

[2] To whom correspondence should be addressed.



0021-9517/91 $3.00

fore use in industrial plants is through model reactions. Catalyst performance can then be investigated by comparing either the activities and selectivities of the various catalysts for a given reaction at a fixed set of reaction conditions or the kinetic parameters obtained from detailed kinetic studies.

In previous work, the effects of deactivation and regeneration on the performance of the catalysts studied here have been investigated using probe reactions to examine each function of the catalyst separately. The metallic function was studied by Pookote (*1*) using cyclohexene hydrogenation under conditions where the acidic function had been selectively (and reversibly) prepoisoned by ammonia while the acidic function was then characterized by Absil (*2, 3*) using cumene transalkylation.

In the present work, the feasibility of pyridine hydrodenitrogenation (HDN) and piperidine hydrogenolysis as probe reactions for characterizing simultaneously both catalyst functions and for determining their possible mutual interactions under reaction conditions has been investigated. The results presented here refer only to the studies using the fresh hydrocracking catalyst (NU-D), a catalyst formulated with the metallic function on silica (AM-1), and the catalyst support (AM-2). Corresponding studies of commercially deactivated and regenerated catalysts are presented subsequently.

When comparing the catalysts on the basis of their kinetic parameters a necessary criterion to be satisfied by the probe reaction is that the characterization should be independent of catalyst deactivation. Three methods for determining the kinetic parameters of a reaction over a deactivating catalyst pertinent to the present study are discussed here.

In the first characterization method, the catalyst is allowed to deactivate to a state where additional deactivation is negligible, and then the kinetic parameters are determined over this steady-state catalyst. The kinetic parameters of pyridine HDN over dual-functional catalysts were determined using this method by several investigators in the past (*4–13*). The steady-state method, however, does not take into account the effects of catalyst aging on parameter estimation. When the hydrocracking catalyst deactivates, its chemical properties change with time on stream as indicated by changes in activity and selectivity. The catalyst physical properties may change as well during the deactivation process as was repeatedly reported in the past (*14–21*). Therefore, correlating the kinetic parameters or catalytic activities determined after a long time on stream to the catalyst chemical and physical properties at zero time on stream can lead to erroneous conclusions (*3*), as demonstrated by the study of Jacobs *et al.* (*22*).

In view of these observations, the determination of the kinetic parameters should be based on initial rate data. This can be achieved by a method in which conversion-time data are extrapolated to zero time on stream via a "Voorhies type" correlation (*23, 24*):

$$\ln(x/x^{o}) = -at^{1/2}. \tag{1}$$

From the initial conversion, an initial rate of reaction can be obtained; however, this extrapolation method is reliable only if the catalyst deactivates slowly. This approach has been successfully used in prior studies with the present and other catalysts (*1–3, 25–27*).

In addition to Eq. (1), another decay correlation can be used to examine catalyst deactivation data and extrapolate to zero time on stream. In particular, Eq. (2) was also reported in the past (*2, 3, 27*) as being successful in correlating experimental data in a differential reactor.

$$x = x^{o}(1 + \beta t)^{-2}. \tag{2}$$

The third method that can be used to determine the kinetic parameters of a reaction over a deactivating catalyst involves the use of a reaction–deactivation model. Levenspiel (*28*) and Wojciechowski (*29*) developed two reaction–deactivation

models. Taking several criteria into consideration, and using the cases of parallel, series, side-by-side, and independent deactivation, Levenspiel (*28*) proposed the following model (see Appendix B for nomenclature):

$$-\frac{dC_A}{dt} = kC_A{}^n\, s$$

$$-\frac{ds}{dt} = k_d\,(C_A,\, C_P,\, C_{PN})^{n^*}\, s^d \qquad (3)$$

$$s = \frac{[dC_A/dt]_t}{[dC_A/dt]_{t=0}}.$$

Krishnaswamy and Kittrell (*30*) and Shum *et al.* (*31, 32*) attempted to use the above model to analyze gas oil hydrocracking data and to correlate data on deactivation by coke formation in *n*-hexane conversion over a $PtRe/Al_2O_3$ catalyst, respectively. After imposing the assumptions of a single irreversible primary reaction and concentration independent deactivation of order one, the resulting simplified equation was able to describe the data of the latter study satisfactorily. However, with these assumptions, a large variation in the activation energy of deactivation was predicted in the former study probably indicative of a model too simple to represent the complicated deactivation mechanisms involved in hydrocracking.

Wojciechowski (*29*) proposed the following reaction–deactivation model (time on stream theory) based on the postulate that catalyst aging is independent of conversion; i.e., it is solely a function of time on stream (*33, 34*):

$$-\frac{dC_A}{dt} = k''[S_o]^{n''} s\; q(C_A)$$

$$-\frac{d}{dt}\,(s^{1/n''}) = \sum_{m=0}^{\infty} k_{md}\, s^{m/n''}. \qquad (4)$$

The kinetic parameters of a reaction over an aging catalyst can be determined using the above model, or the one given by Eqs. (3), when reaction and deactivation mechanisms are postulated.

The time on stream theory, Eqs. (4), as proposed by Wojciechowski, expresses the activity decay as only a function of time. However, coke formation which is one type of catalyst deactivation, is also catalyzed and depends on the concentration of the reacting species; thus aging cannot be a simple function of time (*35*). Catalyst deactivation must hence be expressed by a deactivation function which is related not only to the catalyst operating time, but also to other parameters affecting deactivation, such as the concentration of all coke precursor species. This issue was considered in the present study as discussed further in Appendix A.

Note that Eq. (2) can be derived from the model (4) by assuming $n'' = 2$ and second-order catalyst decay, since in a differential reactor

$$\frac{[dC_A/dt]_t}{[dC_A/dt]_{t=0}} = \frac{x}{x^o} = s. \qquad (5)$$

A different derivation of Eq. (2) is given by Absil *et al.* (*27*) by assuming that during deactivation via coking only the number of active sites changes and not their nature (i.e., separable deactivation) and by applying a differential reactor analysis.

Besides the early approaches to catalyst deactivation that tended to concentrate on empirical correlations (*23, 36, 37*) and in addition to the methods described above, other later developments involving more complex and detailed analyses were also proposed by Froment and Bischoff (*38*) and Corella and Asúa (*39*). In the present work, the steady-state method was used to study the pyridine hydrogenation reaction whereas Eqs. (1) and (3) were employed to correlate the piperidine hydrogenolysis reaction and deactivation rate data.

## EXPERIMENTAL

The catalyst samples used in this work were supplied by Amoco Oil Company. The fresh hydrocracking catalyst, NU-D, contains CoO and $MoO_3$ on a support of ultrastable Y zeolite within a porous matrix

of amorphous silica–alumina. Other catalysts used in this study were AM-1 and AM-2. AM-1 contains CoO and $MoO_3$ supported on Davison 59 silica and AM-2 is a metals-free molecular sieve dispersed in a silica–alumina matrix. In all the experiments reported here, the catalyst samples were crushed and screened to 0.2-mm average particle size.

In the pyridine hydrogenation work the catalyst charge (NU-D) was varied (0.3–0.8 g), depending on reaction conditions, to obtain differential conversion and was pretreated before reaction according to method I. In this method, the catalyst was purged with hydrogen at room temperature for 1 h. It was then heated to 365°C and held at 365°C for 1 h under a flow of hydrogen. A mixture of 10% $H_2S$ in $H_2$ was then passed through the catalyst bed at 40 cc/min (STP) and 365°C until the ratio of the mass of the catalyst to the mass of the $H_2S$ passed was equal to unity. The catalyst was then cooled to room temperature under a flow of hydrogen for 1 h. The kinetic experiments were carried out in a continuous-flow fixed-bed reactor system at temperatures ranging from 312 to 334°C, total pressures of 13.01 to 13.48 atm, and initial pyridine partial pressures of 0.116 to 0.483 atm (remainder was $H_2$). The products formed in the reactions were identified via on-line gas chromatography (GC) and conversion was monitored as a function of time on stream. The reagent pyridine (Fisher Scientific Co., 99.9+%) was used as received. Under the above conditions, transport and thermodynamic (as discussed later) limitations were absent. Further details are given elsewhere (*40*).

In the piperidine hydrogenolysis kinetic experiments the catalyst charge (NU-D) was held constant and equal to 0.5 g. Prior to reaction each catalyst sample was sulfided according to method I*. This method was the same as I except nitrogen was used instead of hydrogen in the two steps prior to the sulfidation step. The reactions were carried out in the same reaction system mentioned above at temperatures ranging from 281 to 321°C, total pressures of 15.86 to 16.14 atm, and initial concentrations of piperidine from 4.03 to 11.84 $\times$ $10^{-3}$ mol/liter. Hydrogen was present in excess and its partial pressure was kept constant. The 95% confidence interval of the hydrogen partial pressure used in the kinetic experiments was $\pm 1\%$. In these experiments space velocities were in the range of 1.07 to 3.57 $h^{-1}$. The products formed in the reactions were identified via on-line GC and by use of off-line GC/MS. Conversion was monitored as a function of time on stream and the reagent piperidine (Fluka Chemical Corp., 99+%) was used as received. Under the above conditions, transport limitations were absent. Further experimental details are given by Hadjiloizou (*41*).

## RESULTS AND DISCUSSION

### *Pyridine Hydrogenation: Product Distribution*

Some prior studies (*4–13, 42–44*) have concluded that the first step in the HDN of pyridine, under high $H_2$ pressure, is the saturation of the heterocyclic ring, followed by ring fracture and subsequent removal of the nitrogen as ammonia,

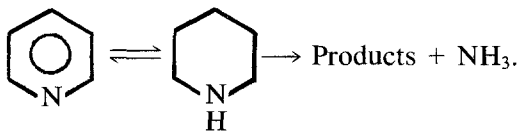


(6)

In the present work, examination of the product distribution of pyridine HDN over the fresh hydrocracking catalyst as a function of time on stream and reaction temperature indicated that pyridine hydrogenation to piperidine was the predominant reaction. Other products such as $C_5$'s and ammonia were also detected but in trace amounts. Long reaction equilibration times, observed under the employed experimental conditions, did not permit the use of the extrapolation-to-zero-time-on-stream method described earlier to characterize the aging

hydrocracking catalyst. To assure that the catalyst characterization was independent of catalyst deactivation and the system had reached "equilibrium," the catalyst was contacted with the pyridine–hydrogen mixture for more than 10 h until a "steady-state" was attained. This steady-state is defined as a state in which the conversion of pyridine to piperidine remained constant with time, and for a time period of 2 h.

A blank experiment was also carried out with a sulfided catalyst containing no metallic function (AM-2) using a pyridine feed at 350°C, total pressure of 11.44 atm, and an initial pyridine partial pressure of 0.146 atm. No conversion was observed during 20 h of operation, indicating that the catalyst metallic sites are responsible for hydrogenation of the pyridine ring.

*Kinetics of Pyridine Hydrogenation*

The effects of temperature and initial pyridine partial pressure on the hydrogenation rate of pyridine were investigated using the fixed-bed reactor system. The space velocity was adjusted such that $x_{pip}$, the conversion of pyridine to piperidine, was always less than 10%. At a particular temperature, pressure, and space velocity, when steady-state was achieved, four or five independent samples were analyzed and their results averaged to obtain a value for conversion. The reaction rate of piperidine formation was calculated using

$$r_{pip} = (F/W)x_{pip}. \tag{7}$$

Reproducibility experiments indicated standard deviations less than 11% for the $r_{pip}$ data as tabulated in Table 1.

In order to find a rate expression for pyridine hydrogenation and to determine the kinetic parameters, a kinetic analysis of these data was performed (*40*) which resulted in best fit to the model described in

$$r_{pip} = k' K_{pyr} P_{pyr} \tag{8}$$

$$k'K_{pyr} = k'^{o} K^{o}_{pyr} \exp(-E_{app}/RT) \tag{9}$$

$$E_{app} = \Delta H_{pyr} + E. \tag{10}$$

In these experiments, the hydrogen partial pressure was kept constant; therefore, its effect on kinetics is included in the rate

TABLE 1

Differential Reaction Rate Data of Pyridine Hydrogenation to Piperidine over the Fresh Hydrocracking Catalyst as Determined by the Steady-State Method

| Reaction temperature (°C) | Space velocity × $10^4$ (mol pyr/g cat/min) | Pyridine partial pressure (atm) | $r_{pip} \times 10^5$ (mol/g cat/min) |
|---|---|---|---|
| 334 | 5.687 | 0.448 | 3.40 |
| 334 | 5.719 | 0.455 | 2.89 |
| 334 | 5.688 | 0.454 | 2.99 |
| 334 | 2.995 | 0.285 | 2.38 |
| 334 | 2.988 | 0.290 | 2.04 |
| 334 | 1.461 | 0.106 | 1.22 |
| 322 | 3.844 | 0.456 | 1.56 |
| 322 | 3.844 | 0.464 | 1.46 |
| 322 | 3.844 | 0.460 | 1.48 |
| 322 | 2.033 | 0.301 | 1.02 |
| 322 | 2.034 | 0.303 | 1.08 |
| 322 | 0.7231 | 0.153 | 0.698 |
| 312 | 2.887 | 0.456 | 1.17 |
| 312 | 1.519 | 0.296 | 0.770 |
| 312 | 0.5459 | 0.153 | 0.515 |

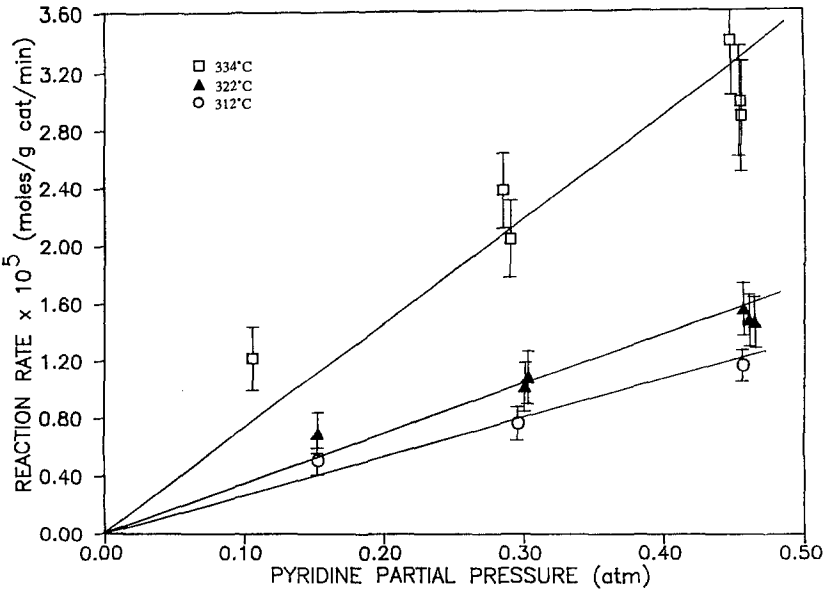


FIG. 1. Change in the hydrogenation rate with the pyridine partial pressure.

constant $k'$ of Eq. (8). A similar rate expression was used by Anabtawi *et al.* (*12*) during pyridine hydrogenation studies over a $NiW/Al_2O_3$ catalyst. In Fig. 1 $r_{pip}$ is plotted as a function of $P_{pyr}$ at 334, 322, and 312°C. The associated kinetic parameters were calculated using the above equations and linear regression and the results are listed in Table 2. The average deviation of the data, $D_{A_r}$, defined as

$$D_{A_r} = (1/i) \sum_i \{[|r_{pip,obs,i} - r_{pip,pred,i}|]/ r_{pip,obs,i}\} (100) \quad (11)$$

was 15%. The above results indicate that Eqs. (8) through (10) can fit the data quite well.

Since most of the steady-state conversions were larger than 5% and Eq. (8) is nonlinear in temperature, it is preferable to estimate the kinetic parameters via an alternative procedure using integral conversion analysis. For plug flow conditions

$$\frac{W}{F} = \int_0^{x_{pip}} \frac{dx_{pip}}{r_{pip}}, \quad (12)$$

where $r_{pip}$ is defined as in Eq. (8). Defining the conversion of pyridine to piperidine as

$$1 - x_{pip} \equiv P_{pyr}/P^o_{pyr} \quad (13)$$

and substituting Eq. (13) into Eq. (12), integration of the resulting expression gives

$$-\frac{F \ln(1 - x_{pip})}{W P^o_{pyr}} = k'^o K^o_{pyr} \exp(-E_{app}/RT). \quad (14)$$

An exponential curve fit of the conversion data to Eq. (14) was performed. The resulting parametric values, which are also reported in Table 2, show good agreement in the activation energies determined from the

TABLE 2

Kinetic Parameters of Pyridine Hydrogenation

| $r_{pip} = k'^o K^o_{pyr} \exp(-E_{app}/RT) P_{pyr}$ | Linear regression | Exponential curve fit |
|---|---|---|
| $E_{app}$ (kcal/mol) | 32.1 ± 1.5 | 34.9 ± 1.5 |
| $k'^o K^o_{pyr}$ (mol/g cat/min/atm) | $2.41 \times 10^7$ | $2.64 \times 10^8$ |
| Coefficient of determination | 0.946 | 0.830 |
| $D_{A_r}$[a](%) | 15 | 16 |

[a] See Eq. (11).

two analyses, but typical variation in preexponential factors. In this case, the average deviation of the data, as calculated from Eq. (11), was 16%. Thus, the two analyses seem equivalent as indicated by the agreement in the parameters listed in Table 2.

*The Pyridine–Piperidine Equilibrium*

Satterfield and Cocchetto (*43*) reported that the equilibrium between pyridine and piperidine can affect the overall rate of reaction if hydrogenolysis of the C–N bond is slower than the hydrogenation of the pyridine ring, and if conditions are such that the equilibrium concentration of piperidine is severely limited. The establishment of the equilibrium of the pyridine to piperidine hydrogenation step depends to a large extent on the experimental conditions. The equilibrium toward piperidine becomes less favorable at higher temperatures and lower hydrogen pressures (*45*).

To determine whether the rate limitation imposed by the ring hydrogenation is thermodynamic or kinetic in nature, the equilibrium constant of the reaction

$$\text{pyridine} + 3H_2 \rightleftharpoons \text{piperidine} \qquad (15)$$

must be known as a function of the experimental conditions employed. It can be shown (*40*) that the reaction potential of this system is given by

$$\Delta G_r = \text{RT ln} \frac{Q}{K_p}, \qquad (16)$$

where $K_p$ is the equilibrium constant of reaction (15) and $Q$ is a pressure function defined by

$$Q = \frac{P_{\text{pip}}}{P_{\text{pyr}}(P_{H_2})^3}. \qquad (17)$$

Thus, if $Q < K_p$, $\Delta G_r$ is negative and the reaction will tend to proceed to the right-hand side (hydrogenation). Therefore, from a knowledge of the equilibrium constant as a function of temperature it is possible to obtain from the kinetic results an indication as to whether or not the pyridine hydrogenation reaction is equilibrium-limited. In the present work, the equilibrium constant $K_p$ was calculated (*40*) based on investigations reported in the literature (*46–49*). The pressure function $Q$ was evaluated at four different temperatures and compared to the estimated values of $K_p$. These results are listed in Table 3 and show that for the first three temperatures (312–334°C), which were used in determination of the kinetic parameters of the hydrogenation reaction, the pressure function was always smaller than $K_p$ by about one order of magnitude.

TABLE 3

The Nature of the Rate Limitation for the Pyridine Hydrogenation Reaction

| Temperature (°C) | 312 | 322 | 334 | 350 |
|---|---|---|---|---|
| Experiment[a] | 34 | 24 | 19 | 3 |
| | Reactor exit | | | |
| $P_{\text{pip}}/P_{\text{pyr}}$ | 0.04221 | 0.05263 | 0.07331 | 0.1270 |
| $P_{H_2}$ (atm) | 12.67 | 12.96 | 12.73 | 11.95 |
| $Q^b$ | $2.077 \times 10^{-5}$ | $2.416 \times 10^{-5}$ | $3.554 \times 10^{-5}$ | $7.438 \times 10^{-5}$ |
| | $K_p$[a] | | | |
| Hales and Herington (*47*) | $1.743 \times 10^{-3}$ | $8.668 \times 10^{-4}$ | $3.864 \times 10^{-4}$ | $1.381 \times 10^{-4}$ |
| McCullough *et al.* (*48*), Scott (*49*) | $2.512 \times 10^{-3}$ | $1.585 \times 10^{-3}$ | $7.943 \times 10^{-4}$ | $3.162 \times 10^{-4}$ |
| Goudriaan (*46*) | $8.219 \times 10^{-4}$ | $4.182 \times 10^{-4}$ | $1.914 \times 10^{-4}$ | $6.894 \times 10^{-5}$ |

[a] Hadjiloizou (*40*).

[b] $Q = P_{\text{pip}}/P_{\text{pyr}}(P_{H_2})^3$

Thus, equilibrium limitations were not a factor. At a temperature of 350°C, however, the data of Goudriaan (*46*) indicate that thermodynamic limitations could have been present within the experimental error range, but other data (*47–49*) still indicate that only kinetic limitations were present at this temperature.

### *The Feasibility of Pyridine HDN as a Probe Reaction*

As stated earlier, the primary purpose of the present study is to investigate pyridine HDN as a probe reaction for characterization of both catalyst functions simultaneously. The above results indicate that the method used for characterizing the aging catalyst was reliable and consistent. However, although the derived rate expression, Eq. (8), can be used to characterize the hydrogenation function of this catalyst in absence of deactivation, the estimated kinetic parameters listed in Table 2 are not necessarily representative of the fresh catalyst due to the steady-state characterization method. They describe rather a catalyst state at which deactivation or any other process occurring on the catalyst surface has reached "equilibrium."

Thus, in order to use the HDN of pyridine as a probe reaction for catalyst characterization, further experiments are required to either show that the catalyst properties are not drastically changing during the duration of the experiments, or to identify other experimental and catalyst pretreatment conditions such that the catalyst deactivates slowly and extrapolation to zero time on stream is possible.

Furthermore, another problem with the pyridine HDN reaction system was the inability to observe a complete HDN product distribution. This was partly due to the limitations imposed by the pyridine–piperidine equilibrium on the employed reaction temperature range (Table 3) and to the total pressure conditions allowed by the reactor system, as discussed elsewhere (*40*). Another reason for this problem could lie in the catalyst pretreatment procedure (method I). In particular, it has been reported (*50*) that when molybdenum catalysts are exposed to hydrogen at high temperature before sulfiding, then the reduced catalyst is not easily sulfided even at temperatures as high as 800°C. Since the catalyst pretreatment procedure for the pyridine hydrogenation experiments included a hydrogen reduction step at 365°C prior to sulfidation, this could have resulted in a catalyst less active for pyridine HDN.

In view of the difficulties encountered with the pyridine hydrogenation reaction, a different reaction was evaluated/chosen for the catalyst characterization work. In particular, the hydrogenolysis of piperidine was employed, which proved to be a feasible probe reaction as discussed next.

### *Piperidine Hydrogenolysis: Product Distribution*

The catalytic hydrogenolysis of piperidine has been carried out under a variety of reaction conditions by many investigators in the past (*4, 9, 44, 51–53*). Many reaction products have been reported of which *N*-*n*-butyl, *N*-*n*-pentyl, *N*-cyclopentyl, and *N*-(5-aminopentyl)-piperidine, 1,5-dipiperidinopentane, *n*-pentylamine, $C_5$'s, ammonia, pyridine, decane, and 4-methylnonane were the most prominent.

The product distributions during piperidine hydrogenolysis over the present sulfided hydrocracking catalyst were examined as a function of time on stream and reaction temperature. The results indicated that a large number of reactions occurred (hydrogenolysis, alkylation, cyclization, cleavage, dehydrogenation, and hydrogenation). At reaction temperatures between 281 and 342°C and hydrogen partial pressures near 14–15 atm several discernible patterns in product distribution were revealed:

(i) Nitrogen was only partially eliminated from piperidine and the predominant reactions were those transforming piperidine to other types of nitrogen compounds.

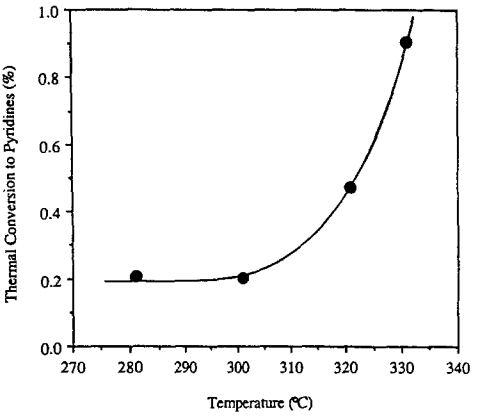


FIG. 2. Thermal conversion of piperidine to pyridines as a function of temperature.

(ii) The alkylation of the heterocyclic ring predominated resulting in the formation of alkylpiperidines with *N*-*n*-pentylpiperidine and 2-*n*-pentylpiperidine as the most prominent.

(iii) Cyclization reactions resulted in the formation of decahydroquinolines, while dehydrogenation of the latter and of piperidine yielded 5,6,7,8-tetrahydroquinoline and pyridines (tetrahydropyridine and pyridine), respectively.

(iv) Formation of unsaturated $C_5$ hydrocarbons and ammonia via hydrogenolysis of both C–N bonds in the piperidine ring also occurred, but to a lesser extent.

(v) Some thermal dehydrogenation of piperidine occurred which yielded mainly tetrahydropyridine and smaller amounts of pyridine. This conversion to pyridines was highly activated by temperature, as shown in Fig. 2. All catalytic conversion data were corrected for this thermal reaction.

(vi) At the reaction conditions under which the kinetic experiments were performed, *N*-*n*-pentylpiperidine, 2-*n*-pentylpiperidine, and decahydroquinolines (decahydroquinoline and methyldecahydroquinoline) were the major products (Fig. 3). Other secondary products were also observed but in smaller concentrations (Fig. 4).

The yield of a product $i$ with respect to reactant piperidine, $Y_i$, is defined as

$$Y_i = \frac{\text{moles of } i \text{ produced}}{\text{moles of piperidine initially}}. \quad (18)$$

A complete listing of the reaction products is given in Table 4 together with their assigned numbers which are used throughout this report.

Although many studies of pyridine and piperidine HDN report alkylation products such as *N*-methyl, *N*-ethyl, *N*-cyclopentyl,

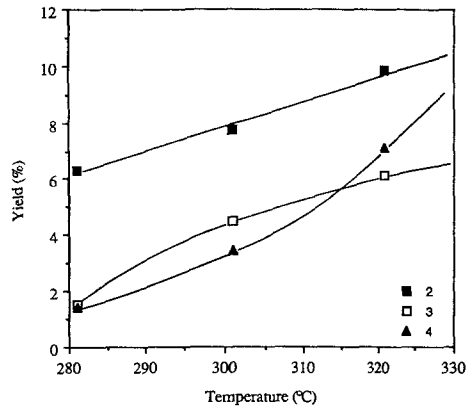


FIG. 3. Yield of the major products in the hydrogenolysis of piperidine on NU-D as a function of temperature at 50 min time on stream; numbers correspond to Table 4.

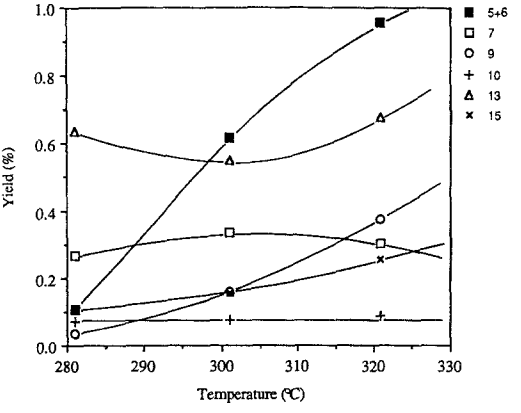


FIG. 4. Yield of the secondary products in the hydrogenolysis of piperidine on NU-D as a function of temperature at 50 min time on stream; numbers correspond to Table 4.

TABLE 4

Number Assignment for Products Formed in the Hydrogenolysis of Piperidine

| Compound | Number |
|---|---|
| Piperidine | 1 |
| *N*-*n*-Pentylpiperidine | 2 |
| 2-*n*-Pentylpiperidine | 3 |
| Decahydroquinolines | 4 |
| Tetrahydropyridine[a] | 5 |
| Pyridine[a] | 6 |
| 2-Pentene + 1,3-pentadiene | 7 |
| *N*-($C_5$ Alkenyl)-piperidine[b] | 8 |
| *N*-Methylpiperidine | 9 |
| *N*-Ethylpiperidine | 10 |
| Compound with MW: 139[c] + *N*-($C_5$ Alkenyl)-piperidine | 11 |
| *N*-($C_5$ Alkenyl)-piperidine[b] + compound with MW: 153[b,c] | 12 |
| *N*-Cyclopentylpiperidine | 13 |
| Compound with MW: 169[c] | 14 |
| 4-*n*-Pentylpyridine + methyltetrahydroquinoline derivative + 5,6,7,8-tetrahydroquinoline | 15 |

[a,b] These could not be separated in GC, therefore they are lumped together as (a) 5 + 6 (pyridines) and (b) 8 + 12.

[c] Compounds identified only by molecular weight.

and *N*-*n*-pentylpiperidine (*5, 9, 11, 12, 44, 46, 51, 53–56*), we have not seen prior reports of the formation of 2-*n*-pentylpiperidine or cyclization products such as quinoline derivatives. Furthermore, the higher yield of alkylpiperidines, especially *N*-*n*-pentylpiperidine, and the lower yield of $C_5$ hydrocarbons obtained in this study as compared to the ones mentioned above reveals the sensitivity of this reaction both to experimental conditions and type of catalyst used. Similar results have been reported by Sonnemans *et al.* (*9*), who show that even at hydrogen partial pressures of about 60 atm with $CoO–MoO_3/Al_2O_3$ the reaction yields almost exclusively ammonia and *N*-*n*-pentylpiperidine with small amounts of $C_5$'s, up to temperatures as high as 350°C. The considerably lower hydrogen partial pressure in the present work would, as discussed elsewhere (*5–10*), favor even higher concentrations of disproportionation products (*N*-*n*-pentylpiperidine) and lower concentrations of hydrocracking products ($C_5$'s).

The presence of the zeolite in the present catalyst could enhance some reactions which on $Al_2O_3$ (used in most prior work) are of secondary importance. It has been suggested (*5*) that the formation of alkylpiperidines (or nitrogen-containing cyclization products) by relatively fast disproportionation (or cyclization) reactions is connected with the high coverage of the catalyst surface with nitrogen bases. Such coverage would be expected to increase with use of highly acidic materials such as Y zeolites. Furthermore, the increase in surface coverage can also be achieved by using catalyst pretreatment procedures (method I*) that modify the catalyst acidity. For example, exposing Mo-containing catalysts to highly reducing environments can lead to the creation of surface vacancies. The Mo cations associated with vacancies are considered to be coordinately unsaturated (*57*) or Lewis acid type centers, and can readily adsorb nitrogen-containing electron-pair donor molecules.

Since Mo- or W-containing catalysts are commercially used for hydrotreating of the products obtained from petroleum and synthetic fuels processing, it is interesting to note that the analyses of the hydrogenation products here (and in some of the other reports) indicate that even at high temperatures nitrogen is only partially eliminated from the heterocyclic molecule. The predominant reactions transform the original molecule to other types of nitrogen compounds, which may then subsequently decompose. Some details of this are given in the following section.

### *A Reaction Scheme for Piperidine Hydrogenolysis*

The sequence of the major reaction steps in the piperidine hydrogenolysis system has been proposed by a number of workers cited above as

piperidine ⇌ pyridine
↓
*n*-pentylamine → ammonia + $C_5$'s
⇃↾ (19)
ammonia + *N*-*n*-pentylpiperidine + di-*n*-pentylamine

However, in this work *n*-pentylamine was not detected and the major reaction products were alkylpiperidines and decahydroquinolines, while secondary products such as pyridines and unsaturated $C_5$'s were also observed. The absence of *n*-pentylamine indicates either that this compound is not an intermediate in the piperidine reactions observed here or that it is so reactive that it is present only in very low concentrations. Regarding the former possibility, reaction mechanisms that do not involve *n*-pentylamine have indeed been proposed (*41, 58–60*) to account for formation of disproportionation products such as *N*-*n*-pentylpiperidine. As far as the latter possibility, McIlvried (*4, 52*) found that the denitrification rate of a primary amine was very fast compared with the denitrification rate of piperidine. Therefore, he concluded that the concentration of the primary amine in the reaction system will always be low. Overall, from the point of view of a practical reaction scheme it would appear that the *n*-pentylamine conversion step can be excluded without affecting the validity of the study.

The formation of unsaturated $C_5$'s, the absence of pentane, and the formation of pyridines are rather surprising since the metal function of commercial hydrocracking catalysts is expected to impart a relatively strong hydrogenation activity. However, the lower overall hydrogenation activity of the catalyst observed here is most probably due to the lower hydrogen partial pressures and somewhat lower temperatures in the present experiments compared to commercial conditions (100–150 atm, 350–450°C).

Figure 5 shows a simplified reaction

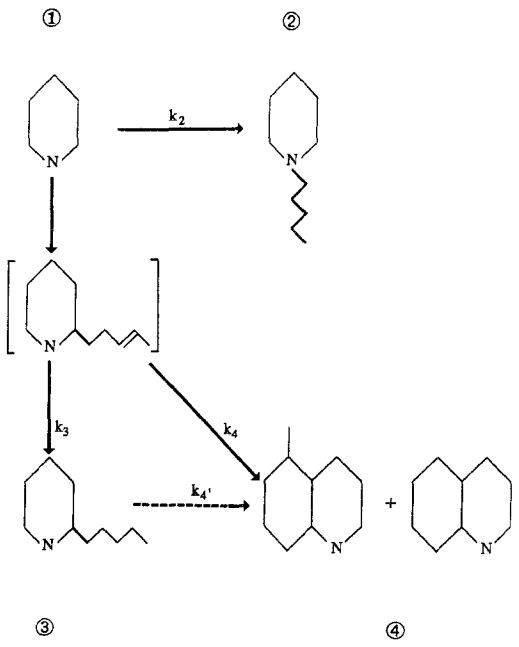


FIG. 5. A simplified reaction scheme for piperidine hydrogenolysis.

scheme for the hydrogenolysis of piperidine on the commercial hydrocracking catalyst that accounts for the major products observed in these lower pressure studies (*41*). It is possible to identify separate contributions of the catalyst functions to the product distribution, as discussed below.

### *Contributions of the Metallic and Acidic Catalyst Functions to the Product Distribution of Piperidine Hydrogenolysis*

To look at the individual contributions of the catalyst functions to the product distribution of piperidine hydrogenolysis, experiments were performed with the fresh catalyst (NU-D), the catalyst acidic support (AM-2), and CoMo on silica of similar metals loading to NU-D (AM-1), under similar conditions. Prior to the experiments, each catalyst was sulfided with a 10% $H_2S$/$H_2$ mixture at 365°C (method I*). The reaction conditions were 301°C, about 15 atm total pressure, and 0.2 atm initial piperidine partial pressure (remainder $H_2$).

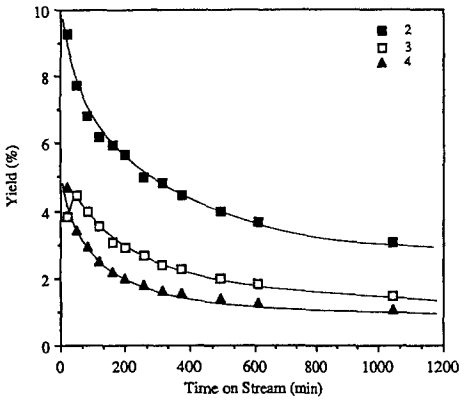


FIG. 6. Yield of the major products in the hydrogenolysis of piperidine on NU-D at 301°C as a function of time on stream; numbers correspond to Table 4.

The product distribution for NU-D is shown in Figs. 6 and 7 as a function of time on stream. The identification of reaction products is tabulated in Table 4. The yield of the major products (**2, 3,** and **4**) decreases with time on stream, with product **3** first going through a maximum. This maximum is strong evidence that this compound is an intermediate in the formation of product **4,** as shown in Fig. 5, via a cyclization reaction. The rest of the yield data for NU-D seems without major patterns; some secondary products decrease with time on stream, others increase (Fig. 7). In addition to the products shown in Fig. 7, small amounts of products **8, 12, 14,** and **15** were detected with no special trend with time on stream.

The experiments with the catalyst acidic support (AM-2) showed that the yield of product **2** was very low, and the primary product was **4** (Fig. 8). Product **3** was not detected, but instead small amounts of a methyldecahydroquinoline isomer were identified. The secondary product distributions are shown in Fig. 9; only very small amounts of pyridines (**5** + **6**), and of products **7** and **15** were detected, while product **11** was formed in substantial quantities. Products **8, 12,** and **14** were again detected in small amounts. In the case of the acidic support function alone, catalyst deactivation is relatively rapid for both major and secondary products (see $Y_4$ and $Y_{11}$). This is expected since it is suggested (61) that one of the roles of the metal hydrogenation sites is to keep the acidic sites active (coke free) by hydrogenating the coke precursors.

The product distributions obtained with the CoMo/silica (AM-1) are shown in Figs. 10 and 11. As with NU-D, the primary product was **2** accompanied with a substantial amount of product **3**. However, no

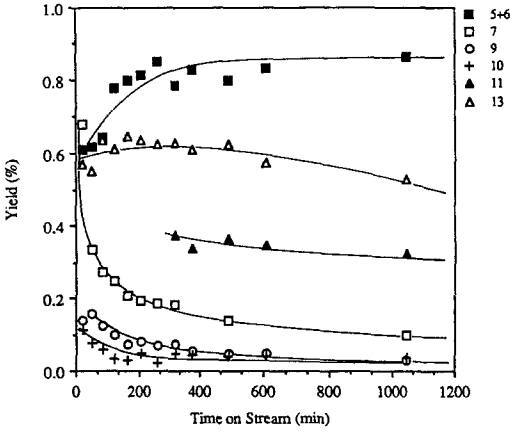


FIG. 7. Yield of the secondary products in the hydrogenolysis of piperidine on NU-D at 301°C as a function of time on stream; numbers correspond to Table 4.

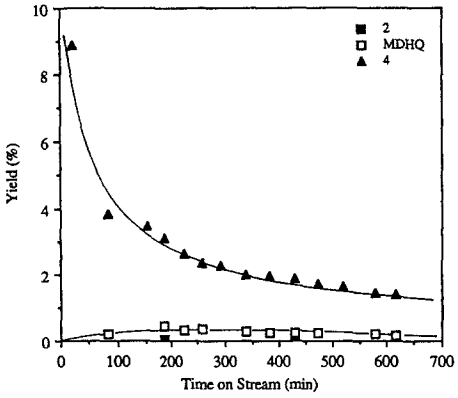


FIG. 8. Yield of the major products in the hydrogenolysis of piperidine on AM-2 at 301°C as a function of time on stream; MDHQ is a methyldecahydroquinoline isomer; numbers correspond to Table 4.

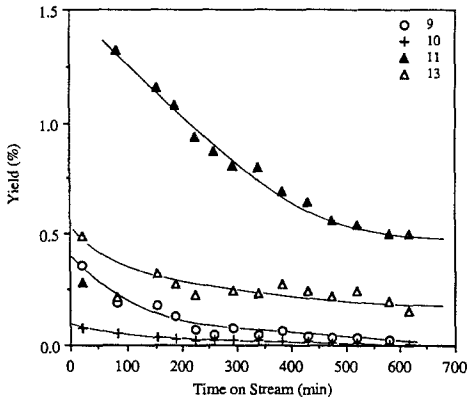


FIG. 9. Yield of the secondary products in the hydrogenolysis of piperidine on AM-2 at 301°C as a function of time on stream; numbers correspond to Table 4.

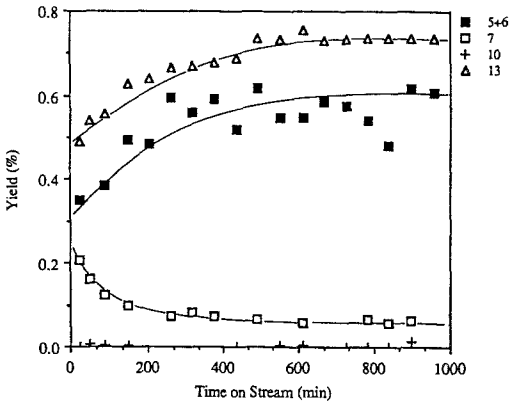


FIG. 11. Yield of the secondary products in the hydrogenolysis of piperidine on AM-1 at 301°C as a function of time on stream; numbers correspond to Table 4.

maximum in the yield of product **3** was observed, possibly indicating shorter equilibration times on the $SiO_2$. The yield of product **4** was much lower than that for either NU-D or the acidic support, while products **5, 6,** and **7** were formed in appreciable amounts on the CoMo/silica catalyst but not on the support. Products **9, 11,** and **14** were detected in trace amounts while small amounts of products **8, 12,** and **15** were also observed. Product **13** was formed on all three catalysts, but demonstrates a distinctive time on stream behavior with each, passing through a maximum on NU-D, decreasing on the acidic support, and increasing on CoMo/silica.

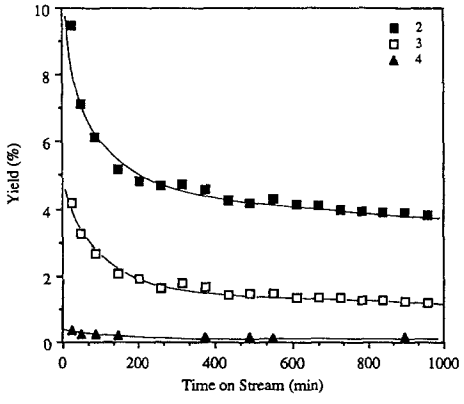


FIG. 10. Yield of the major products in the hydrogenolysis of piperidine on AM-1 at 301°C as a function of time on stream; numbers correspond to Table 4.

A number of conclusions can be drawn from these comparative experiments in light of the proposals of Fig. 5:

(i) The formation of *N*-*n*-pentylpiperidine (**2**) and 2-*n*-pentylpiperidine (**3**) can be attributed exclusively to the metallic catalyst function.

(ii) 2-*n*-Pentylpiperidine (**3**) apparently undergoes a cyclization reaction on neighboring metal sites of the catalyst to form decahydroquinolines (**4**), but only to a limited extent (i.e., $k_{4'} \approx 0$ in Fig. 5). Thus, the acidic catalyst function is mainly responsible for the cyclization reaction to form product **4**.

(iii) Dehydrogenation of piperidine to pyridines (**5** + **6**) occurs on both metal and acidic catalyst sites, but to a lesser extent on the latter.

(iv) Pyridines (**5** + **6**) or an intermediate of the dehydrogenation step participate in another reaction whose rate decreases with time on stream, hence the increase in $Y_{5+6}$ with time.

(v) *N*-Cyclopentylpiperidine (**13**) is formed on both catalyst functions, possibly via two different mechanisms.

(vi) The acidic function is mainly responsible for the formation of *N*-methylpiperidine (**9**) and product **11**.

(vii) The products **7, 8, 10, 12, 14,** and **15** appear to be formed on both catalyst functions; there is some preferential activity of the metal for product **7**.

(viii) Overall, under the established experimental conditions both catalyst functions are active simultaneously, and the observations on product distributions are generally in accord with the proposed scheme of Fig. 5.

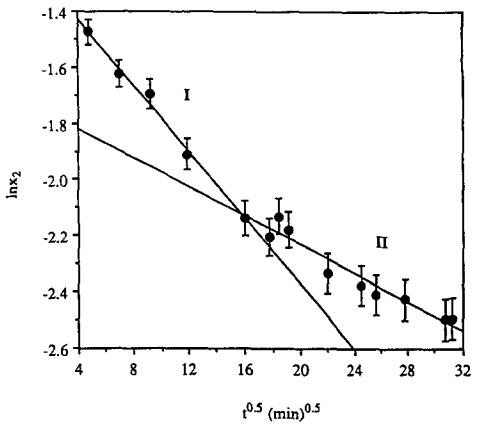


FIG. 12. Plot of ln $x_2$ versus $t^{0.5}$ for NU-D at 321°C, total pressure of 15.98 atm, and initial concentration of piperidine of $4.03 \times 10^{-3}$ mol/liter.

*Catalyst Characterization Method: Extrapolation to Zero Time on Stream*

The results presented above verify that the piperidine hydrogenolysis reaction has the desired property of bifunctionality. Under the established experimental and catalyst pretreatment conditions, both the metallic and acidic catalyst functions are active simultaneously. Although the complete spectrum of the piperidine hydrogenolysis product distribution has been identified, the emphasis of the present study is placed on the formation of the three major products, namely *N*-*n*-pentylpiperidine (**2**), 2-*n*-pentylpiperidine (**3**), and decahydroquinolines (**4**). The formation of these products involves, as desired, both the metallic and acidic catalyst functions. As shown in Fig. 6, the activity of both functions of the fresh hydrocracking catalyst decreases with time on stream. Thus, for the analysis of reaction kinetics it is important, as mentioned earlier, to find a method which provides a reliable working basis for the determination of initial activity levels.

The experimental conversion of piperidine to products **2, 3,** and **4,** as defined by Eq. (20), was correlated to time on stream via the "Voorhies type" correlation, as shown by Eq. (21).

$$x_i = \frac{\text{moles of piperidine reacted to } i}{\text{moles of piperidine initially}} \quad (20)$$

$$x_i(t) = x_i(0)\exp(-a_i t^{0.5}). \quad (21)$$

Typical results for product **2** from an experiment at 321°C, a total pressure of 15.98 atm, and an initial concentration of piperidine of $4.03 \times 10^{-3}$ mol/liter are shown in Fig. 12, where the linearized form (Eq. (1)) of the decay correlation was employed. Products **3** and **4** follow the same general pattern. For all three products, the deactivation was occurring in two distinct regimes (regions I and II) with a rapid initial step followed by a more gradual activity decline. Similar behavior was also observed when the total conversion of piperidine, $x_t$, was fit to Eq. (21), as shown in Fig. 13. Other workers have also reported the presence of two regimes of deactivation (*1, 25, 32, 62, 63*) and various speculations were cited to explain this type of behavior. Regimes I and II are sometimes referred to as "fast" and "slow" coke respectively, and they have been proposed to correspond to the initial deposition of a carbonaceous layer with considerable $C^+$ character, followed by the dehydrogenation and transformation of the layer to more graphitic structures (*32*). Another explanation for the two regimes of deactivation observed, was reported by Absil (*3*) who proposed that regions I and II correspond to the deactivation of two types of catalytic sites

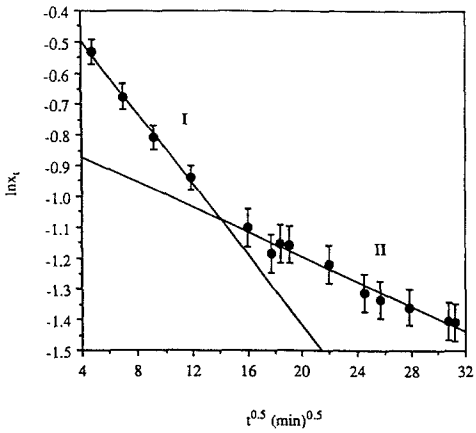


FIG. 13. Plot of ln $x_t$ versus $t^{0.5}$ for NU-D at 321°C, total pressure of 15.98 atm, and initial concentration of piperidine of $4.03 \times 10^{-3}$ mol/liter.

with different activity. Various aspects of the above speculations as well as specifics related to the deactivation process are reported separately in part II of this work now in preparation.

The linear plots indicate that the decay correlation managed to fit the experimental data very well. Further experimental reproducibility results indicated that the average deviations of the parameters associated with Eq. (21), as calculated by an expression similar to Eq. (11), are as listed in Table 5. Although for the catalyst characterization work only the results from region I (data in absence of deactivation) were used, the deviation of parameters in region II is also included for completeness. The data clearly show good experimental reproducibility and are within acceptable deviations, especially in region I. Therefore, under the typical conditions used in the present study, the catalyst deactivation is slow enough and the extrapolation to zero time on stream technique is reliable and consistent. The decay correlation (Eq. (21)) was used to determine the initial conversions and decay parameters during the piperidine hydrogenolysis kinetic experiments, as discussed next.

TABLE 5

Experimental Reproducibility: The Average Deviation of Reaction Parameters in the Hydrogenolysis of Piperidine

| Parameter | Average deviation (%) | |
|---|---|---|
| | Region I | Region II |
| $x_i^\circ$ | 11.8 | 20.8 |
| $a_i$ | 7.4 | 6.3 |
| $k_i^\circ$ | 14.4 | 16.1 |

*Kinetics of Piperidine Hydrogenolysis*

The kinetics of piperidine hydrogenolysis and the formation of products **2, 3,** and **4** over the fresh catalyst (NU-D) were studied at different temperatures and initial concentrations of piperidine to determine the effects of these parameters on the reaction and deactivation rates. At reaction temperatures higher than 321°C the catalyst deactivation was very fast and extrapolation to zero time on stream was questionable while at temperatures below 281°C the system exhibited long initial equilibration times interfering with the extrapolation technique. Thus, the experimental conditions mentioned earlier were chosen.

For each experiment, the conversions $(x_t, x_2, x_3, x_4)$ versus time on stream were fit to the decay correlation and the initial conversions and decay parameters were determined. In all cases two deactivation regions were observed, as illustrated in Figs. 12 and 13. The conversion data were then fit to the reaction–deactivation model described by Eqs. (22)–(25), and the kinetic parameters of piperidine hydrogenolysis were obtained.

$$\frac{1}{k_t^\circ \tau} + \frac{k_{d_t}^* t}{k_t^\circ \tau} = \left(\frac{1 - x_t}{x_t}\right) \tag{22}$$

$$k_{d_t}^* = k_{d_t} C_{1_o}{}^{n^*} \tag{23}$$

$$k_{i\mathrm{I}}^\circ = \frac{x_{i\mathrm{I}}^\circ}{x_{t\mathrm{I}}^\circ} k_{t\mathrm{I}}^\circ \tag{24}$$

$$k_{i\mathrm{II}}^\circ = \frac{x_{i\mathrm{II}}^\circ}{x_{t\mathrm{II}}^\circ} k_{t\mathrm{II}}^\circ. \tag{25}$$

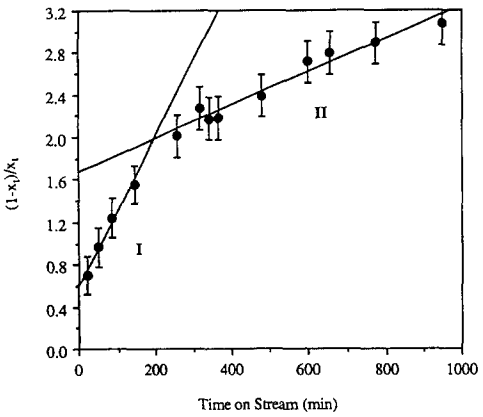


FIG. 14. Plot of $(1 - x_t)/x_t$ versus time on stream for NU-D; conditions as for Figs. 12 and 13.

Detailed derivation of this model is given in Appendix A. The correlation of the data according to Eq. (22) for a typical piperidine hydrogenolysis experiment (see conditions for Figs. 12 and 13) is shown in Fig. 14. For each region $k_i^\circ$ and $k_{d_i}^*$ were determined via linear analysis, and Eqs. (24) and (25) were then used to calculate $k_{i\mathrm{I}}^\circ$ and $k_{i\mathrm{II}}^\circ$ for products **2, 3,** and **4**. The results of this analysis are given in Tables 6 and 7. Although the parameters from region I are mostly used in subsequent catalyst characterization work, the results obtained from both regions are reported here for completeness. Experimental reproducibility results, reported in Table 5, indicate average deviations of the reaction parameters $k_i^\circ$ of less than ±17%. The linearity of the experimental data according to Eq. (22) supports the assumption of separability on the reaction–deactivation kinetics of the scheme in Fig. 5 and verifies the viability of the rest of the approach used in Appendix A.

*Effects of initial concentration of piperidine.* At a fixed temperature and different initial concentrations of piperidine, Eq. (23) indicates that a ln–ln plot of $k_{d_t}^*$ versus $C_{\mathrm{I}_o}$ should be linear with a slope equal to the order of concentration dependency of deactivation. Such analysis of the results listed in Table 6 is shown in Fig. 15 and the corre-

TABLE 6

Reaction and Deactivation Parameters of Piperidine Hydrogenolysis on Sulfided NU-D at 301°C

| | | | |
|---|---|---|---|
| Space velocity × $10^4$ (mol pip/g cat/min) | 2.099 | 4.547 | 6.995 |
| Total pressure (atm) | 15.86 | 16.14 | 16.10 |
| Initial concentration of piperidine × $10^3$ (mol/liter) | 4.14 | 8.11 | 11.84 |
| | Region I[a] | | |
| $k_{r\mathrm{I}}^\circ$ | 7.99 | 4.09 | 2.63 |
| $k_{d\mathrm{I}}^* \times 10^3$ (min)$^{-1}$ | 5.68 | 9.78 | 14.70 |
| $k_{2\mathrm{I}}^\circ$ | 3.32 | 1.96 | 1.30 |
| $k_{3\mathrm{I}}^\circ$ | 2.09 | 1.02 | 0.663 |
| $k_{4\mathrm{I}}^\circ$ | 1.64 | 0.826 | 0.607 |
| | Region II[a] | | |
| $k_{r\mathrm{II}}^\circ$ | 4.10 | 1.59 | 0.910 |
| $k_{d\mathrm{II}}^* \times 10^3$ (min)$^{-1}$ | 0.776 | 0.937 | 0.823 |
| $k_{2\mathrm{II}}^\circ$ | 2.12 | 0.689 | 0.333 |
| $k_{3\mathrm{II}}^\circ$ | 1.03 | 0.276 | 0.124 |
| $k_{4\mathrm{II}}^\circ$ | 0.624 | 0.222 | 0.125 |

[a] $k_i^\circ$ in liter²/mol/g cat/min.

TABLE 7

Reaction and Deactivation Parameters of Piperidine Hydrogenolysis on Sulfided NU-D as a Function of Temperature

| | | | |
|---|---|---|---|
| Reaction temperature (°C) | 281 | 301 | 321 |
| Space velocity × $10^4$ (mol pip/g cat/min) | 2.099 | 2.099 | 2.099 |
| Total pressure (atm) | 16.10 | 15.86 | 15.98 |
| Initial concentration of piperidine × $10^3$ (mol/liter) | 4.35 | 4.14 | 4.03 |
| | Region I[a] | | |
| $k_{r\mathrm{I}}^\circ$ | 3.25 | 7.99 | 21.93 |
| $k_{d\mathrm{I}}^* \times 10^3$ (min)$^{-1}$ | 2.04 | 5.68 | 12.08 |
| $k_{2\mathrm{I}}^\circ$ | 2.01 | 3.32 | 8.68 |
| $k_{3\mathrm{I}}^\circ$ | 0.687 | 2.09 | 5.29 |
| $k_{4\mathrm{I}}^\circ$ | 0.406 | 1.64 | 7.27 |
| | Region II[a] | | |
| $k_{r\mathrm{II}}^\circ$ | 2.14 | 4.10 | 7.56 |
| $k_{d\mathrm{II}}^* \times 10^3$ (min)$^{-1}$ | 0.590 | 0.776 | 0.874 |
| $k_{2\mathrm{II}}^\circ$ | 1.27 | 2.12 | 2.99 |
| $k_{3\mathrm{II}}^\circ$ | 0.497 | 1.03 | 2.09 |
| $k_{4\mathrm{II}}^\circ$ | 0.251 | 0.624 | 1.44 |

[a] $k_i^\circ$ in liter²/mol/g cat/min.

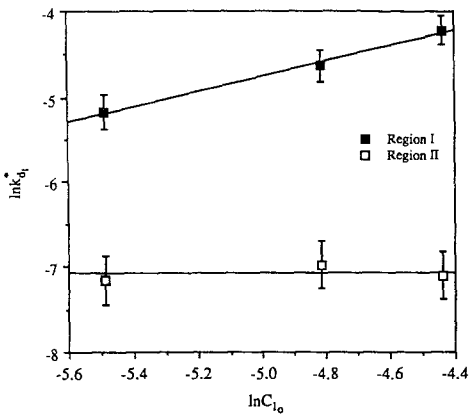


FIG. 15. Change in the apparent overall deactivation rate constant with the initial concentration of piperidine for NU-D at 301°C.

sponding deactivation parameters are reported in Table 8. The order of concentration dependency of deactivation is about 1 in region I while the data in region II indicate that deactivation is independent of $C_{l_o}$. The good correlation observed between catalyst deactivation and initial concentration of piperidine in region I justifies the use of ${C_{l_o}}^{n^*}$ as the concentration-dependent term of the catalyst activity decline rate, as discussed in Appendix A. By definition, the concentration of all components present which can contribute to deactivation (formation of coke precursors) should be included in the concentration-dependent term $\Phi(C)$. However, as shown above, the replacement of the component concentrations in $\Phi(C)$ with $C_{l_o}$ is most reasonable.

To determine the reaction and deactivation parameters listed in Tables 6 and 7, Eq. (26) was employed as a rate expression for piperidine hydrogenolysis in the derivation of the reaction–deactivation model (see Appendix A).

$$(-r_l) = k_t^{\circ} {C_l}^2 s_t. \tag{26}$$

However, piperidine as well as the N-containing intermediate and/or product molecules are expected to be relatively strongly adsorbed on the catalyst surface, and possibly exhibit a self-inhibition behavior. Such systems can usually be adequately described by means of Langmuir–Hinshelwood kinetics (*64*). In the present case, analysis of the reaction data (*41*) resulted in best fit to the expression

$$(-r_l) = \frac{k_t^{o''} {K_{\text{pip}_t}}^2 {C_l}^2 s_t}{(1 + K_{\text{pip}_t} C_{l_o})^2}. \tag{27}$$

Thus,

$$k_t^{o} = \frac{k_t^{o''} {K_{\text{pip}_t}}^2}{(1 + K_{\text{pip}_t} C_{l_o})^2}. \tag{28}$$

Since the hydrogen partial pressure was fixed in any set of experiments here, its effect on kinetics is embedded in $k_t^{o''}$. Further discussion on the effects of hydrogen partial pressure will be given in a later report. A simple linear analysis of Eq. (28) suggests that a plot of $1/\sqrt{k_t^{o}}$ versus the initial concentration of piperidine should be linear, and this is so as shown in Fig. 16. The re-

TABLE 8

Deactivation Parameters of Piperidine Hydrogenolysis on Sulfided NU-D at 301°C

| Parameter | Region I | Region II |
|---|---|---|
| $n^*$ | 0.894 | ~0 |
| $k_{d_t}$ | 0.756[a] | $0.845 \times 10^{-3}$[b] |
| $R^2$ | 0.994 | |

[a] liter/mol/min.
[b] $(1/i)\ \Sigma_i\ (k_{d_{\text{III}}}^*)_i$ min$^{-1}$.

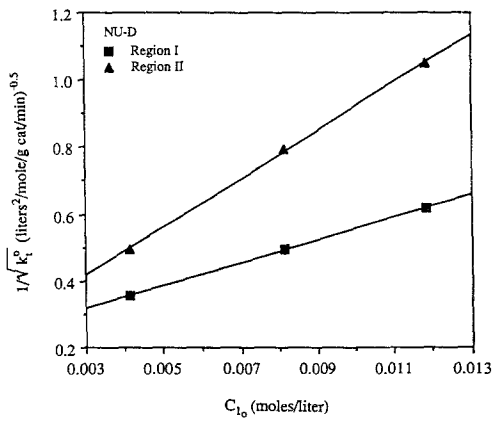


FIG. 16. Plot of $1/\sqrt{k_t^{o}}$ versus $C_{l_o}$ at 301°C.

TABLE 9

Reaction Kinetic Parameters of Piperidine Hydrogenolysis on Sulfided NU-D at 301°C

| $(-r_1)$ and $r_i = \frac{k_i^{o\prime\prime} K_{pip_i}^2 C_1^2 s_i}{(1 + K_{pip_i} C_{1_o})^2}$ [a] | Region I | Region II |
|---|---|---|
| $k_t^{o\prime\prime}$ | 8.54 | 1.93 |
| | [1.000][b] (0.91%)[c] | [0.999] (1.5%) |
| $K_{pip_t}$ | 160.3 | 361.3 |
| $k_2^{o\prime\prime}$ | 5.47 | |
| | [1.000] (0.55%) | |
| $K_{pip_2}$ | 115.6 | |
| $k_3^{o\prime\prime}$ | 2.05 | |
| | [0.998] (2.1%) | |
| $K_{pip_3}$ | 170.7 | |
| $k_4^{o\prime\prime}$ | 2.35 | |
| | [0.982] (5.2%) | |
| $K_{pip_4}$ | 123.1 | |

[a] $k_i^{o\prime\prime}$ in mol/g cat/min × $10^4$, $K_{pip_i}$ in liter/mol.
[b] Coefficient of determination for regression analysis.
[c] Average deviation (see Eq. (11)).

sulting parameters are reported in Table 9. In both regions, average deviations from the overall reaction data with Eq. (27) are less than ±1.6%. An expression similar to Eq. (28) was also used to correlate the initial reaction rate constants of formation of products **2, 3,** and **4**. Although in region I a good fit was again observed, as shown in Fig. 17 and reported in Table 9, the deviations associated with region II were much larger (*41*) and the corresponding parameters could not be accurately determined.

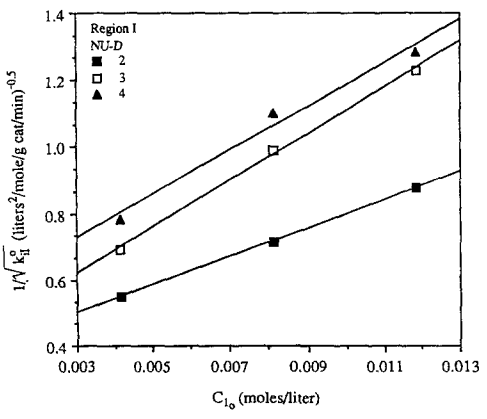


FIG. 17. Plot of $1/\sqrt{k_{iI}^o}$ versus $C_{1_o}$ at 301°C.

The different behavior of the reaction data in the two regions indicated above and the different deactivation dependency of the two regions on $C_{1_o}$ as discussed earlier seem to indicate that the reaction–deactivation kinetics in regions I and II are not the same. However, the values of the kinetic parameters for the formation of products **2, 3,** and **4** as calculated using Eq. (28) in region II should be regarded with caution. The calculation procedure for $k_{iII}^o$ and in particular the assumption of $s_{iII} = s_{tII}$ in the derivation of Eq. (25) in Appendix A is questionable. As mentioned earlier the deactivation process affects not only the activity of the catalyst but also the selectivity since the functions of the hydrocracking catalyst deactivate at different rates. Hence, the values of $s_{iII}$ are most probably not equal to $s_{tII}$ and the parameters calculated for products **2, 3,** and **4** in region II using an expression such as Eq. (25) are not necessarily the intrinsic values but rather the latter multiplied by the factor $s_{iII}/s_{tII}$.

A rate expression similar to Eq. (27) was

also proposed by Catry and Jungers (*65*) during disproportionation reaction studies some time ago. However, more elaborate models have also been reported for amine disproportionation studies (*66*) that attempt to distinguish between the kinetics on acidic and basic sites. These, though, become so highly parameterized that it is doubtful whether the result is worth the effort.

*Surface coverage.* Since inhibition effects are apparently of importance in the kinetic correlation here, it is worth examining the initial surface coverage of the catalyst with the strongly adsorbed nitrogen-containing molecules involved in the piperidine hydrogenolysis reaction. From the Langmuir adsorption isotherm relationship (*64*) it follows that

$$\theta_N = \frac{K_N C_N}{1 + K_N C_N}. \tag{29}$$

Then,

$$\theta_V = 1 - \theta_N \tag{30}$$

or

$$\theta_V = \frac{1}{1 + K_N C_N}. \tag{31}$$

If we make the assumption that the total concentration of all adsorbed nitrogen compounds, at any time, is essentially equal to the initial concentration of piperidine, i.e.,

$$K_N C_N = K_{\text{pip}_t} C_{l_o}, \tag{32}$$

then combining Eqs. (31) and (32) with Eq. (28) yields

$$k_t^o = k_t^{o''} K_{\text{pip}_t}{}^2 \theta_V^2, \tag{33}$$

which allows computation of $\theta_V$ and thence $\theta_N$ at given conditions (*67*). Equation (33) was employed in the present work and values of $\theta_N$ were calculated at 301°C and various initial concentrations of piperidine, for region I of the data. The results are listed in Table 10 and shown in Fig. 18. The increase in initial surface coverage and subsequent saturation with increasing piperidine feed concentration is typical of a reaction subject to self-inhibition. Note that this result is based on experimentally determined parameters.

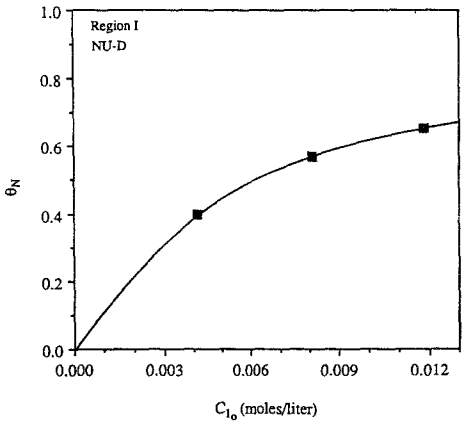


FIG. 18. Initial catalyst surface coverage as a function of initial concentration of piperidine in region I at 301°C.

*Effects of temperature.* A simple Arrhenius type analysis of the data for the overall deactivation in the hydrogenolysis of piperidine yields for $k_{d_t}^*$ (see Appendix A and Eq. (23))

$$\ln k_{d_t}^* = \ln B - \left(\frac{E_{d_t}}{RT}\right), \tag{34}$$

where $B = k'_{d_t} C_{l_o}{}^{n^*}$. The correlation of the data in Table 7 using the above equation is shown in Fig. 19 for both regions I and II. The corresponding parameters, as listed in Table 11, indicate that deactivation is much

TABLE 10

Initial Catalyst[a] Surface Coverage in the Hydrogenolysis of Piperidine at 301°C[b]

| $C_{l_o} \times 10^3$ (mol/liter) | $k_{rl}^o$ (liter²/mol/g cat/min) | $\theta_N$ |
|---|---|---|
| 4.14 | 7.99 | 0.40 |
| 8.11 | 4.09 | 0.57 |
| 11.84 | 2.63 | 0.65 |

[a] Sulfided NU-D.

[b] $k_{rl}^{o''} = 8.54 \times 10^{-4}$ mol/g cat/min. $K_{\text{pip}_{rl}} = 160.3$ liter/mol.

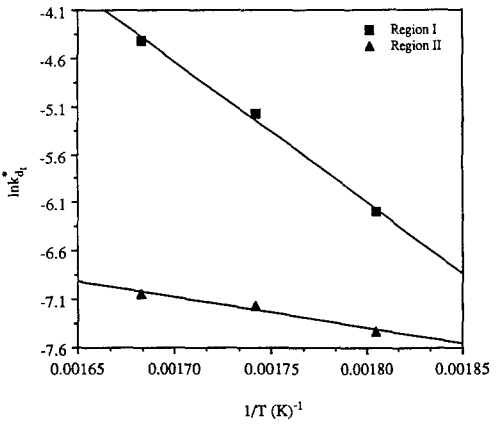


FIG. 19. Arrhenius plot to determine the activation energy of overall deactivation in the hydrogenolysis of piperidine on NU-D.

more temperature-sensitive in region I than in region II.

Using the results in Table 11 for region I and the Arrhenius type form of $k_{d_t}$ (see Appendix A), the overall deactivation rate constant can be calculated at any temperature within the range examined in this work. For example, at 301°C a value for $k_{d_{tI}}$ equal to 0.711 liters/mole/min is obtained. This is in excellent agreement with the $k_{d_{tI}}$ value calculated earlier from the experiments at 301°C, as shown in Table 8. A similar calculation using the results for region II yields a value for $k_{d_{tII}}$ at 301°C equal to $0.740 \times 10^{-3}$ min$^{-1}$, which is in good agreement with the earlier result also shown in Table 8.

TABLE 11

Arrhenius Type Overall Deactivation Parameters for Sulfided NU-D

| Parameter | Region I[a] | Region II[b] |
|---|---|---|
| $E_{d_t}$ (kcal/mol) | 29.1 | 6.5 |
| $B$ (min)$^{-1}$ | $6.53 \times 10^{8}$ | 0.215 |
| $k'_{d_t}$ | $8.77 \times 10^{10}$[c] | 0.215[d] |

[a] $R^2 = 0.996$.
[b] $R^2 = 0.960$.
[c] Using $\overline{C}_{1_0} = 4.18 \times 10^{-3}$ mol/liter, $n^* = 0.894$, in liter/mol/min.
[d] Assuming $n^* = 0$, in min$^{-1}$.

For analysis of the temperature dependence of the various reaction steps a more extensive set of data are required than that reported here in order to evaluate $k_i^{o''}$ and $K_{\text{pip}_i}$ individually and to determine the corresponding activation energies and heats of adsorption. However, overall we may look at the dependence of $k_t^o$ and $k_i^o$ on temperature with an Arrhenius type correlation such as

$$\ln k_i^o = \ln A_i - \left(\frac{E_i}{RT}\right). \tag{35}$$

Linear regression indicated that Eq. (35) could correlate the data in both regions, as listed in Table 7, quite well. A typical plot of the data is shown in Fig. 20 and all the results are tabulated in Table 12. It is interesting that the apparent activation energies show a progressive increase as one goes from product **2** to **4**. $E_t$, of course, reflects only the overall value for the formation of all products.

*Reaction mechanism for piperidine disproportionation.* It is possible to propose a detailed reaction mechanism for piperidine disproportionation consistent with the experimentally determined correlation, Eq.

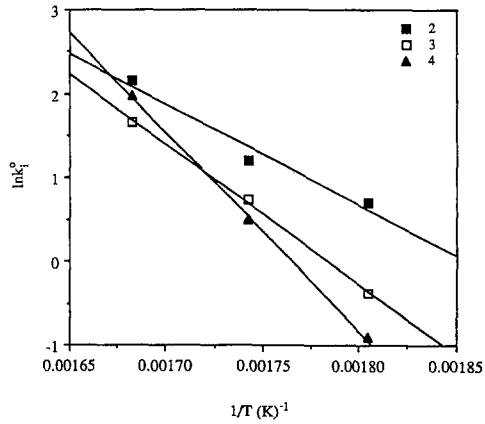


FIG. 20. Arrhenius plots to determine the activation energy of formation of products **2**, **3**, and **4**, on NU-D in region I.

TABLE 12

Arrhenius Type Reaction Kinetic Parameters for Sulfided NU-D

| Parameter[a] | Region I | Region II |
|---|---|---|
| $E_t$ | 31.2 | 20.6 |
| $A_t$ | $6.34 \times 10^{12}$ | $2.88 \times 10^{8}$ |
| $R_t^2$ | 0.997 | 1.000 |
| $E_2$ | 23.8 | 14.0 |
| $A_2$ | $4.60 \times 10^{9}$ | $4.26 \times 10^{5}$ |
| $R_2^2$ | 0.961 | 0.992 |
| $E_3$ | 33.4 | 23.5 |
| $A_3$ | $1.05 \times 10^{13}$ | $9.13 \times 10^{8}$ |
| $R_3^2$ | 0.999 | 1.000 |
| $E_4$ | 47.2 | 28.6 |
| $A_4$ | $1.58 \times 10^{18}$ | $4.73 \times 10^{10}$ |
| $R_4^2$ | 0.998 | 1.000 |

[a] $E_i$ in kcal/mol, $A_i$ in liter²/mol/g cat/min.

(27), and the overall scheme of Fig. 5. The *N-n*-pentylpiperidine formation will be used as an example while similar mechanisms hold for the formation of the other products. In detail, the mechanism postulates that two piperidine molecules are adsorbed on adjacent catalytic sites and react together with dissociatively adsorbed hydrogen to form *N-n*-pentylpiperidine. In this Langmuir–Hinshelwood mechanism two different sites are involved for hydrogen and organocompound adsorption. It has also been proposed (*41*) that the two sites adsorbing the reacting piperidine molecules are different, consisting of an acidic and a basic site. However, for simplicity the sites adsorbing piperidine are denoted $S_1$ while the sites adsorbing hydrogen are denoted $S_2$. The latter could possibly be the sulfur ions bonded to Mo (*41*). The sequence would then be

(i) $2[\text{Pip} + S_1 \rightleftharpoons \text{Pip}\text{–}S_1]$, $K^*_{\text{pip}_2}$

(ii) $H_2 + 2S_2 \rightleftharpoons 2\text{H}\text{–}S_2$, $K_{H_2}$

(iii) $2\text{Pip}\text{–}S_1 + 2\text{H}\text{–}S_2 \rightarrow \text{PPip}\text{–}S_1 + \text{NH}_3\text{–}S_1 + 2S_2$, $k_2^*$(r.l.s.) (36)

(iv) $\text{PPip}\text{–}S_1 \rightleftharpoons \text{PPip} + S_1$, $K_{\text{ppip}}$

(v) $\text{NH}_3\text{–}S_1 \rightleftharpoons \text{NH}_3 + S_1$, $K_{\text{NH}_3}$.

Assuming that the surface reaction forming *N-n*-pentylpiperidine and $NH_3$ is the rate-limiting step, then $r_2$ can be written as

$$r_2 = \frac{k_2^*(K^*_{\text{pip}_2})^2 N_1^2 K_{H_2} N_2^2 P_{\text{pip}}{}^2 P_{H_2}}{(1 + K^*_{\text{pip}_2}P_{\text{pip}} + K_{\text{ppip}}P_{\text{ppip}} + K_{\text{NH}_3}P_{\text{NH}_3})^2} \times \frac{1}{(1 + K_{H_2}{}^{1/2}P_{H_2}{}^{1/2})^2}. \quad (37)$$

At a constant hydrogen partial pressure, the assumptions of identical adsorption equilibrium constants for the nitrogen bases and low coverage of hydrogen result in

$$r_2 = \frac{k_2''(K^*_{\text{pip}_2})^2 P_{\text{pip}}{}^2}{(1 + K^*_{\text{pip}_2}P^{\circ}_{\text{pip}})^2}, \quad (38)$$

where

$$k_2'' = k_2^* N_1^2 N_2^2 K_{H_2} P_{H_2}. \quad (39)$$

When Eq. (38) is written in concentration units it becomes equivalent to Eq. (27) written for product **2**. Equation (39) indicates the importance of keeping the hydrogen partial pressure constant when determining the kinetic parameters of piperidine hydrogenolysis. To ascertain the effect of hydrogen on the reactions here, experiments at a constant piperidine partial pressure and varying hydrogen partial pressures were performed, as discussed separately in part II of these reports.

The concerted reaction involved in (iii) above is unlikely; however, since piperidine is expected to adsorb strongly on the catalyst surface, the piperidine surface coverage should be high enough (see Fig. 18) to result in rapid equilibration among a number of surface species favoring association and subsequent bimolecular reaction. However, although the proposed mechanism yields the experimentally determined kinetic rate expression, this does not mean to imply that the actual mechanism for this reaction has been identified but rather that a useful kinetic equation was found which may have some theoretical basis.

*The Feasibility of Piperidine Hydrogenolysis as a Probe Reaction*

A primary purpose of the present study was to ascertain the feasibility of piperidine hydrogenolysis as a probe reaction for simultaneous characterization of both catalyst functions. Affirmative evidence has been found. Specifically, the piperidine hydrogenolysis reaction exhibits the desired property of bifunctionality. In particular, under the established reaction conditions the formation of the three major products, *N*-*n*-pentylpiperidine, 2-*n*-pentylpiperidine, and decahydroquinolines, involves the participation of both catalyst functions simultaneously. Furthermore, extrapolation to zero time on stream and application of the reaction–deactivation model resulted in kinetic data which were successfully fit to a kinetic model that can be derived from theoretical principles. Therefore, in the present experiments catalyst deactivation is slow enough so that extrapolation to zero time on stream is reliable and consistent as indicated by the agreement of the kinetic model with the experimental data and the experimental reproducibility.

## CONCLUSIONS

(i) Piperidine hydrogenolysis is a feasible probe reaction for characterization studies of dual-functional catalysts because it exhibits the property of bifunctionality and catalyst deactivation is slow enough to permit accurate extrapolation to zero time on stream.

(ii) The pyridine hydrogenation reaction is successfully correlated with a first-order rate expression. However, pyridine hydrogenation is less preferable as a probe reaction because of the steady-state method used to characterize the aging hydrocracking catalyst and the inability to observe a wide HDN product distribution.

(iii) Kinetic analysis suggests that piperidine hydrogenolysis proceeds by a type of Langmuir–Hinshelwood reaction sequence involving two adjacently adsorbed piperidine molecules.

(iv) Catalyst deactivation proceeds in two well-defined regions corresponding to time on stream. In the first region (I), the deactivation rate is roughly proportional to the initial concentration of piperidine and has an apparent activation energy of 29.1 ± 0.2 kcal/mol. The second region (II) is much less activated by temperature (6.5 ± 0.2 kcal/mol) and the rate of deactivation is essentially independent of the initial concentration of piperidine.

(v) The reaction–deactivation model employed for determining the reaction and deactivation parameters of piperidine hydrogenolysis is reliable and consistent.

(vi) Overall, the major reactions of piperidine hydrogenolysis on Co–Mo/zeolite catalysts consist of conversion to other nitrogen-containing hydrocarbons of various types. Complete (or substantial) conversion to ammonia and hydrocarbons requires more severe conditions and higher conversions than those investigated here.

## APPENDIX A

*Reaction–Deactivation Model for Piperidine Hydrogenolysis*

Following the early work on deactivation by Szépe and Levenspiel (*68*), the reaction rate in a catalytic system can be described by an equation of the following general form:

$$r = r(\text{present conditions, past history}). \quad \text{(A-1)}$$

Thus, the reaction rate at a given moment will not be just a function of the present operating conditions, but also of the entire past history of the catalyst. To simplify Eq. (A-1) the effects of past history are usually separated from those of the present conditions to yield the product of two terms as shown by Eq. (A-2); one term depends solely on the present conditions (reaction term) and the other solely on the past history (activity term).

$$r = r^{\circ}(\text{present conditions}) \cdot \rho(\text{past history}). \quad \text{(A-2)}$$

Szépe and Levenspiel called form (A-2) of the rate equation "separable."

Using the initial catalyst condition as a reference state, the activity of the catalyst, $s$, at conditions ($T$, $C$) and at time on stream $t$, is defined by

$$s(T, C, t) = \frac{r(T, C, t)}{r(T, C, 0)}. \qquad \text{(A-3)}$$

This definition applies to all deactivation processes, irrespective of whether the rate equation is separable or not. In the case of separable rate equation,

$$s = \rho \qquad \text{(A-4)}$$

and then

$$r = r^{o}(T, C) \cdot s \qquad \text{(A-5)}$$

or

$$r = k^{o}(T) \cdot f(C) \cdot s. \qquad \text{(A-6)}$$

Under the conditions of separability, the kinetics of the reaction are regarded to be unchanged by deactivation and the activity variation can be studied independently of the reaction term (*68*).

Equation (A-6) is not valid for all systems, being only a specific case of the more general form, Eq. (A-1). For example, Butt *et al.* (*69*) pointed out that the concept of separability has been widely used for interpretation of deactivation by coking, but the use of separable factors for the effect of deactivation on the reaction kinetics where chemical poisoning is the decay mechanism has led to difficulty in various studies. Furthermore, in their analysis of deactivation kinetics for a number of model surfaces, Butt *et al.* (*69*) concluded that formulation in terms of a separable activity factor is correct only for an ideal surface composed of sites that all have the same properties and catalytic activity. Thus, to explain the successful correlation of the data when assuming separable deactivation during a cumene disproportionation study on a commercial hydrocracking catalyst, Absil *et al.* (*27*) proposed the following idea. The catalyst surface is initially heterogeneous and nonideal but is undergoing a modification during the deactivation process. Many factors can be responsible for this change, including the preferential deactivation of the most active sites, which will leave the surface progressively less heterogeneous, i.e., more ideal. Regardless of the reason, Eq. (A-6) has been shown and is expected to be a satisfactory first approximation for many systems (*68*). Therefore, separable deactivation has also been assumed in the present work.

To determine the kinetic parameters of piperidine hydrogenolysis over the commercial hydrocracking catalyst, a simplified reaction scheme is written as shown in Fig. 5, according to which the rates of formation of these major products are given by

$$r_1 = -k_2^{o}C_1^{n}s_2 - k_3^{o}C_1^{n}s_3 - k_4^{o}C_1^{n}s_4 \qquad \text{(A-7)}$$

$$r_2 = k_2^{o}C_1^{n}s_2 \qquad \text{(A-8)}$$

$$r_3 = k_3^{o}C_1^{n}s_3 - k_{4'}^{o}C_3^{n'}s_{4'} \qquad \text{(A-9)}$$

$$r_4 = k_4^{o}C_1^{n}s_4 + k_{4'}^{o}C_3^{n'}s_{4'}, \qquad \text{(A-10)}$$

where $k_{4'}^{o} \approx 0$ as discussed in the text and assuming the concentration-dependent terms are of the form shown above. A more general form for the overall rate of disappearance of piperidine (**1**) can be written as

$$(-r_1) = k_t^{o}C_1^{n}s_t. \qquad \text{(A-11)}$$

In general, the rate of change of catalyst activity is a function of operating and catalyst conditions

$$\left(-\frac{ds_t}{dt}\right) = \xi(T, C, s_t), \qquad \text{(A-12)}$$

which is often written in a separable form as

$$\left(-\frac{ds_t}{dt}\right) = k_{d_t}(T) \cdot \Phi(C) \cdot \Psi(s_t). \qquad \text{(A-13)}$$

For equations such as (A-13) the effects of temperature, concentration, and activity can be individually examined. The temperature-dependent term can be of the Arrhenius type

$$k_{d_t}(T) = k'_{d_t} \exp(-E_{d_t}/\mathrm{RT}). \qquad \text{(A-14)}$$

The concentration-dependent term of Eq. (A-13) is in its simplest form a power function

$$\Phi(C) = \left(\sum_p C_p\right)^{n^*} \qquad \text{(A-15)}$$

and all components present (reactant, products, and especially poisons) may contribute to deactivation. A special case is when $n^* = 0$; thus

$$\Phi(C) = 1 \qquad \text{(A-16)}$$

and the deactivation is then called concentration-independent. In the present work, the summation of the concentration terms in Eq. (A-15) is replaced by the initial concentration of piperidine, $C_{1_o}$; therefore

$$\Phi(C) = {C_{1_o}}^{n^*}. \qquad \text{(A-17)}$$

The activity-dependent term of Eq. (A-13) can be written as a simple power function, namely,

$$\Psi(s_t) = {s_t}^d. \qquad \text{(A-18)}$$

Substituting Eqs. (A-17) and (A-18) into Eq. (A-13) yields

$$\left(-\frac{ds_t}{dt}\right) = k_{d_t} {C_{1_o}}^{n^*} {s_t}^d. \qquad \text{(A-19)}$$

At a fixed temperature and initial concentration of piperidine

$$\left(-\frac{ds_t}{dt}\right) = k^*_{d_t} {s_t}^d, \qquad \text{(A-20)}$$

where $k^*_{d_t} = k_{d_t} {C_{1_o}}^{n^*}$. Next, Eqs. (A-11) and (A-20) should in principle be solved simultaneously to determine the various reaction and deactivation parameters. In practice, it is simpler to assume different orders of reaction, $n$, and of deactivation, $d$, and to test the experimental data against the resulting expressions. Then the set of $n$, $d$ that results in the best fit of the data is chosen. The data of the present study were best fit by $n = d = 2$.

For $d = 2$, integration of Eq. (A-20) yields

$$s_t = (1 + k^*_{d_t} t)^{-1} \qquad \text{(A-21)}$$

since $s_t = 1$ at $t = 0$. For a fixed-bed reactor with plug flow of fluid and constant volumetric flow rate, substitution of Eq. (A-11) gives

$$\frac{W}{F_{1_o}} = \int_0^{x_t} \frac{dx_t}{(-r_1)} = -\frac{1}{k_t^o C_{1_o} s_t} \int_{C_{1_o}}^{C_1} \frac{dC_1}{C_1^2}. \qquad \text{(A-22)}$$

Upon integration

$$\frac{W C_{1_o}^2}{F_{1_o}} = \tau = \frac{1}{k_t^o s_t}\left(\frac{x_t}{1 - x_t}\right) \qquad \text{(A-23)}$$

is obtained. Combining with Eq. (A-21) the above correlation can be transformed to the final form

$$\frac{1}{k_t^o \tau} + \frac{k^*_{d_t} t}{k_t^o \tau} = \left(\frac{1 - x_t}{x_t}\right). \qquad \text{(A-24)}$$

The initial reaction rate constants of formation of products **2, 3,** and **4** (Fig. 5) can be determined as follows. For $k^o_{4'} = 0$ and $n = 2$, the rate of formation of each of these products is given by

$$r_i = k_i^o C_1^2 s_i = (\text{mol of } \mathbf{1} \text{ to } i/\text{g cat/min}) \qquad \text{(A-25)}$$

and the overall rate of disappearance of piperidine is written as

$$(-r_1) = k_t^o C_1^2 s_t = (\text{mol of } \mathbf{1} \text{ reacted/g cat/min}). \qquad \text{(A-26)}$$

Taking the ratio of Eq. (A-25) to Eq. (A-26) yields

$$\frac{r_i}{(-r_1)} = \frac{k_i^o s_i}{k_t^o s_t}. \qquad \text{(A-27)}$$

At $t = 0$, $s_i = s_t = 1$; thus,

$$\frac{r_i^o}{(-r_1^o)} = \frac{k_i^o}{k_t^o} = \left(\frac{\text{mol of } \mathbf{1} \text{ to } i}{\text{mol of } \mathbf{1} \text{ reacted}}\right)_{t=0}. \qquad \text{(A-28)}$$

Considering the definition of conversion $x_i$ given earlier, Eq. (A-28) can be written as

$$k_{i\mathbf{1}}^o = \frac{x_{i\mathbf{1}}^o}{x_{t\mathbf{1}}^o} k_{t\mathbf{1}}^o, \qquad \text{(A-29)}$$

where subscript I refers to region I of deactivation and the initial conversions are determined as discussed in the text. The value of $k_{tI}^{o}$ is estimated from region I data using Eq. (A-24). At $t \neq 0$

$$k_i^o = \frac{x_i s_t}{x_t s_i} k_t^o. \qquad \text{(A-30)}$$

If $s_{iII} = s_{tII}$, then Eq. (A-30) can be employed to estimate the initial rate constants in region II, $k_{iII}^{o}$, by using the corresponding parameters of this region. However, there is no reason in general that this restriction is necessarily followed. Note that only $k_{iI}^{o}$ and $k_{tI}^{o}$ are the "true" initial rate constants, i.e., in the absence of deactivation.

## APPENDIX B: NOMENCLATURE

| | |
|---|---|
| $A_i$ | Parameter used in Eq. (35) for overall reaction and for products **2, 3,** and **4,** liter$^2$/mol/g cat/min. |
| $a$ | Empirical parameter in Voorhies type correlation. |
| $a_i$ | Decay parameter for the formation of product $i$, min$^{-0.5}$. |
| $B$ | Parameter used in Eq. (34), min$^{-1}$. |
| $C$ | Set of concentration of all components. |
| $C_A$ | Concentration of reactant $A$. |
| $C_N$ | Total nitrogen concentration. |
| $C_P$ | Concentration of $P$, a product of reaction of $A$. |
| $C_p$ | Concentration of $p$. |
| $C_{PN}$ | Concentration of PN, a poison. |
| $C_l$ | Concentration of piperidine, mol/liter. |
| $C_{l_o}$ | Initial concentration of piperidine, mol/liter. |
| $\overline{C}_{l_o}$ | Initial average concentration of piperidine, mol/liter. |
| $D_{A_i}$ | Average deviation of $i$. |
| $d$ | Order of deactivation. |
| $E$ | Activation energy of pyridine hydrogenation, kcal/mol. |
| $E_{app}$ | Apparent activation energy of pyridine hydrogenation, kcal/mol. |
| $E_{d_t}$, $E_i$, $E_t$ | Activation energy of overall deactivation, formation of product $i$, and overall reaction, respectively, kcal/mol. |
| $F$ | Reactor inlet molar flow rate of pyridine, gmol/min. |
| $F_{l_o}$ | Reactor inlet molar flow rate of piperidine, gmol/min. |
| $f(C)$ | Function of the set of concentration of all components. |
| $i$ | Index. |
| $K_{H_2}$, $K_N$, $K_{NH_3}$ | Adsorption equilibrium constant for hydrogen, overall nitrogen, and ammonia, respectively. |
| $K_p$ | Reaction equilibrium constant. |
| $K_{pip_i}$, $K_{pip_t}$ | Adsorption equilibrium constant for piperidine associated with formation of product $i$ and overall reaction, respectively, liter/mol. |
| $K_{pip_2}^{*}$ | Adsorption equilibrium constant for piperidine used in reaction mechanism (36), atm$^{-1}$. |
| $K_{ppip}$ | Adsorption equilibrium constant for *N*-*n*-pentylpiperidine. |
| $K_{pyr}$ | Adsorption equilibrium constant for pyridine, atm$^{-1}$. |
| $K_{pyr}^{o}$ | Preexponential factor of $K_{pyr}$, atm$^{-1}$. |
| $k$ | Rate constant of reaction of $A$. |
| $k^o$ | Initial reaction rate constant. |
| $k'$ | Rate constant of pyridine hydrogenation, mol/g cat/min. |
| $k'^o$ | Preexponential factor of $k'$, mol/g cat/min. |
| $k''$ | Rate constant per active site. |
| $k_d$ | Rate constant of deactivation reaction. |
| $k_{d_t}$ | Rate constant of overall deactivation reaction, liter/mol/min or min$^{-1}$. |
| $k'_{d_t}$ | Preexponential factor of $k_{d_t}$, liter/mol/min or min$^{-1}$. |
| $k_{d_t}^{*}$ | Apparent rate constant of overall deactivation reaction, min$^{-1}$. |

$k^*_{d_{\mathrm{I}}}$, $k^*_{d_{\mathrm{II}}}$ Apparent rate constant of overall deactivation reaction in region I and II, respectively, $\mathrm{min}^{-1}$.

$k_i$ Reaction rate constant of formation of product $i$ as defined in Fig. 5.

$k_i^{\circ}$, $k_i^{\circ\prime\prime}$ Initial reaction rate constants of formation of product $i$, $\mathrm{liter}^2/\mathrm{mol/g\ cat/min}$ and $\mathrm{mol/g\ cat/min}$, respectively.

$k_{i\mathrm{I}}^{\circ}$, $k_{i\mathrm{II}}^{\circ}$ Initial reaction rate constant of formation of product $i$ in region I and II, respectively, $\mathrm{liter}^2/\mathrm{mol/g\ cat/min}$.

$k_{md}$ Rate constant of deactivation reaction.

$k_t^{\circ}$, $k_t^{\circ\prime\prime}$ Initial rate constants of overall reaction, $\mathrm{liter}^2/\mathrm{mol/g\ cat/min}$ and $\mathrm{mol/g\ cat/min}$, respectively.

$k_{t\mathrm{I}}^{\circ}$, $k_{t\mathrm{II}}^{\circ}$ Initial rate constant of overall reaction in region I and II, respectively, $\mathrm{liter}^2/\mathrm{mol/g\ cat/min}$.

$k_2^*$ Forward rate constant of the rate-limiting step for the formation of *N-n*-pentylpiperidine as defined in reaction mechanism (36).

$k_2''$ Rate constant for the formation of *N-n*-pentylpiperidine.

MDHQ Methyldecahydroquinoline isomer.

$m$ Number of sites in the rate-determining step of the deactivation reaction.

$N_1$, $N_2$ Total number of active sites $S_1$ and $S_2$, respectively.

$n$, $n'$ Orders of reaction with respect to reactant concentration.

$n^*$ Order of concentration dependency of deactivation.

$n''$ Order of reaction with respect to site concentration.

$P_{\mathrm{H_2}}$ Partial pressure of hydrogen, atm.

Pip Piperidine.

$P_{\mathrm{NH_3}}$ Partial pressure of ammonia.

PPip *N-n*-Pentylpiperidine.

$P_{\mathrm{pip}}$, $P_{\mathrm{ppip}}$ Partial pressure of piperidine and *N-n*-pentylpiperidine, respectively.

$P_{\mathrm{pip}}^{\circ}$ Initial partial pressure of piperidine.

$P_{\mathrm{pyr}}$ Partial pressure of pyridine, atm.

$P_{\mathrm{pyr}}^{\circ}$ Initial partial pressure of pyridine, atm.

$p$ Index.

$Q$ Pressure function defined in Eq. (17).

$q(C_A)$ Function of reactant $A$ concentration.

$R$ Gas constant, kcal/mol/K.

$R^2$ Coefficient of determination for regression analysis.

$R_i^2$, $R_t^2$ Coefficient of determination for regression analysis associated with formation of product $i$ and overall reaction, respectively.

$r$ Catalytic reaction rate.

$r^{\circ}$ Initial catalytic reaction rate.

$r_i$ Reaction rate of formation of product $i$, mol/g cat/min.

$r_{\mathrm{pip}}$ Reaction rate of pyridine hydrogenation to piperidine, mol/g cat/min.

$(-r_1)$ Overall rate of disappearance of piperidine, mol/g cat/min.

$[S_o]$ Initial concentration of active sites.

$S_1$, $S_2$ Active sites 1 and 2, respectively.

$s$ Activity of catalyst at time on stream $t$.

$s_i$, $s_t$ Activity of catalyst at time on stream $t$ for formation of product $i$ and overall reaction, respectively.

$s_{i\mathrm{II}}$, $s_{t\mathrm{II}}$ Activity of catalyst at time on stream $t$ in region II for formation of product $i$ and overall reaction, respectively.

$T$ Absolute temperature, $K$.

$t$ Time on stream, min.

| | |
|---|---|
| $W$ | Weight of catalyst, g. |
| $x$ | Conversion at time on stream $t$. |
| $x^{\circ}$ | Conversion at zero time on stream-initial conversion. |
| $x_i$ | Conversion of piperidine to product $i$ at time on stream $t$. |
| $x_i^{\circ}$ | Initial conversion of piperidine to product $i$. |
| $x_{i\mathrm{I}}^{\circ}$, $x_{i\mathrm{II}}^{\circ}$ | Initial conversion of piperidine to product $i$ in region I and II, respectively. |
| $x_{\mathrm{pip}}$ | Conversion of pyridine to piperidine at steady-state. |
| $x_t$ | Total conversion of piperidine at time on stream $t$. |
| $x_{t\mathrm{I}}^{\circ}$, $x_{t\mathrm{II}}^{\circ}$ | Initial total conversion of piperidine in region I and II, respectively. |
| $Y_i$ | Yield of product $i$ with respect to reactant piperidine. |

*Greek Symbols*

| | |
|---|---|
| $\beta$ | Empirical constant. |
| $\Delta G_r$ | Reaction potential defined in Eq. (16), kcal/mol. |
| $\Delta H_{\mathrm{pyr}}$ | Enthalpy change of adsorption of pyridine, kcal/mol. |
| $\theta_{\mathrm{N}}$ | Fractional surface coverage with organic nitrogen. |
| $\theta_V$ | Fraction of surface not covered with organic nitrogen. |
| $\xi$ | Function of operating and catalyst conditions. |
| $\rho$ | Function of catalyst past history. |
| $\tau$ | Parameter defined in Appendix A. |
| $\Phi(C)$ | Function of the set of concentration of all components contributing to catalyst deactivation. |
| $\Psi(s_t)$ | Function of catalyst activity for overall reaction. |

ACKNOWLEDGMENTS

This research was supported by Amoco Oil Company. We thank R. J. Bertolacini and L. C. Gutberlet of Amoco for the catalyst samples. The assistance of Dr. Hoying Hung at the Chemistry Analytical Laboratory of Northwestern University is appreciated.

REFERENCES

1. Pookote, S. R., Ph.D. dissertation, Northwestern University, Evanston, IL, 1980.
2. Absil, R. P. L., M.S. thesis, Northwestern University, Evanston, IL, 1982.
3. Absil, R. P. L., Ph.D. dissertation, Northwestern University, Evanston, IL, 1984.
4. McIlvried, H. G., *Ind. Eng. Chem. Process Des. Dev.* **10** (1), 125 (1971).
5. Sonnemans, J., Goudriaan, F., and Mars, P., *in* "Proceedings, 5th International Congress on Catalysis, Palm Beach, 1972" (J. W. Hightower, Ed.), Vol. 2, p. 1085. North-Holland, Amsterdam, 1973.
6. Sonnemans, J., van den Berg, G. H., and Mars, P., *J. Catal.* **31,** 220 (1973).
7. Sonnemans, J., and Mars, P., *J. Catal.* **31,** 209 (1973).
8. Sonnemans, J., and Mars, P., *J. Catal.* **34,** 215 (1974).
9. Sonnemans, J., Neyens, W. J., and Mars, P., *J. Catal.* **34,** 230 (1974).
10. Sonnemans, J., Janus, J. M., and Mars, P., *J. Phys. Chem.* **80** (19), 2107 (1976).
11. Gupta, R. K., Mann, R. S., and Gupta, A. K., *J. Appl. Chem. Biotechnol.* **28,** 641 (1978).
12. Anabtawi, J. A., Mann, R. S., and Khulbe, K. C., *J. Catal.* **63,** 456 (1980).
13. Hanlon, R. T., *Energy Fuels* **1** (5), 424 (1987).
14. Ramser, J. H., and Hill, P. B., *Ind. Eng. Chem.* **50** (1), 117 (1958).
15. Appleby, W. G., Gibson, J. W., and Good, G. M., *Ind. Eng. Chem. Process Des. Dev.* **1** (2), 102 (1962).
16. Beuther, H., and Schmid, B. K., *in* "Proceedings, 6th World Petroleum Congress, Frankfurt," Section III, p. 297. Hamburg, 1963.
17. Butt, J. B., Delgado-Diaz, S., and Muno, W. E., *J. Catal.* **37,** 158 (1975).
18. Stanulonis, J. J., Gates, B. C., and Olson, J. H., *AIChE J.* **22** (3), 576 (1976).
19. Prasher, B. D., Gabriel, G. A., and Ma, Y. H., *Ind. Eng. Chem. Process Des. Dev.* **17** (3), 266 (1978).
20. Langner, B. E., *Ind. Eng. Chem. Process Des. Dev.* **20** (2), 326 (1981).
21. Wolf, E. E., and Alfani, F., *Catal. Rev. -Sci. Eng.* **24** (3), 329 (1982).
22. Jacobs, P. A., Declerck, L. J., Vandamme, L. J., and Uytterhoeven, J. B., *J. Chem. Soc. Faraday 1* **71,** 1545 (1975).
23. Voorhies, A., Jr., *Ind. Eng. Chem.* **37** (4), 318 (1945).
24. Butt, J. B., and Petersen, E. E., "Activation, De-

activation, and Poisoning of Catalysts." Academic Press, San Diego, 1988.
25. Mahoney, J. A., *J. Catal.* **32,** 247 (1974).
26. Corma, A., Fornés, V., Perez-Pariente, J., Sastre, E., Martens, J. A., and Jacobs, P. A., *in* "Perspectives in Molecular Sieve Science" (W. H. Flank, and T. E. Whyte, Jr., Eds.), Am. Chem. Soc. Symposium Series, Vol. 368, p. 555. Am. Chem. Soc., Washington, DC, 1988.
27. Absil, R. P. L., Butt, J. B., and Dranoff, J. S., *J. Catal.* **85,** 415 (1984).
28. Levenspiel, O., *J. Catal.* **25,** 265 (1972).
29. Wojciechowski, B. W., *Catal. Rev. -Sci. Eng.* **9** (1), 79 (1974).
30. Krishnaswamy, S., and Kittrell, J. R., *Ind. Eng. Chem. Process Des. Dev.* **18** (3), 399 (1979).
31. Shum, V. K., Ph.D. dissertation, Northwestern University, Evanston, IL, 1985.
32. Shum, V. K., Sachtler, W. M. H., and Butt, J. B., *Ind. Eng. Chem. Res.* **26** (7), 1280 (1987).
33. Wojciechowski, B. W., *Can. J. Chem. Eng.* **46,** 48 (1968).
34. Pachovsky, R. A., Best, D. A., and Wojciechowski, B. W., *Ind. Eng. Chem. Process Des. Dev.* **12** (3), 254 (1973).
35. Derouane, E. G., *in* "Catalysis by Acids and Bases" (B. Imelik *et al.,* Eds.), Studies in Surface Science and Catalysis, Vol. 20, p. 221. Elsevier, Amsterdam, 1985.
36. Maxted, E. B., and Stone, V., *Chem. Soc. London J.,* 26 (1934).
37. Hougen, O. A., and Watson, K. M., "Chemical Process Principles: Kinetics and Catalysis," p. 886. Wiley, New York, 1947.
38. Froment, G. F., and Bischoff, K. B., *Chem. Eng. Sci.* **16,** 189 (1961).
39. Corella, J., and Asúa, J. M., *Ind. Eng. Chem. Process Des. Dev.* **21** (1), 55 (1982).
40. Hadjiloizou, G. C., M.S. thesis, Northwestern University, Evanston, IL, 1986.
41. Hadjiloizou, G. C., Ph.D. dissertation, Northwestern University, Evanston, IL, 1989.
42. Goudriaan, F., Gierman, H., and Vlugter, J. C., *J. Inst. Pet.* **59** (565), 40 (1973).
43. Satterfield, C. N., and Cocchetto, J. F., *AIChE J.* **21** (6), 1107 (1975).
44. Černý, M., *Collect. Czech. Chem. Commun.* **44,** 85 (1979).
45. Cocchetto, J. F., and Satterfield, C. N., *Ind. Eng. Chem. Process Des. Dev.* **15** (2), 272 (1976).
46. Goudriaan, F., Doctoral thesis, Twente Technical Institute, The Netherlands, 1974.
47. Hales, J. L., and Herington, E. F. G., *Trans. Faraday Soc.* **53,** 616 (1957).
48. McCullough, J. P., Douslin, D. R., Messerly, J. F., Hossenlopp, I. A., Kincheloe, T. C., and Waddington, G., *J. Am. Chem. Soc.* **79,** 4289 (1957).
49. Scott, D. W., *J. Chem. Thermodyn.* **3,** 649 (1971).
50. Zabala, J. M., Grange, P., and Delmon, B., *C. R. Acad. Sci. Ser. C* **279,** 725 (1974), as cited in Yang, S. H., and Satterfield, C. N., *J. Catal.* **81,** 168 (1983).
51. Jones, J. I., *J. Chem. Soc.,* 1392 (1950).
52. McIlvried, H. G., *Prepr.-Am. Chem. Soc., Div. Pet. Chem.* **15,** A33 (1970).
53. Schulz, H., Schon, M., and Rahman, N. M., *in* "Catalytic Hydrogenation" (L. Červený, Ed.), Studies in Surface Science and Catalysis, Vol. 27, p. 201. Elsevier, Amsterdam, 1986.
54. Beugeling, T., Boduszyński, M., Goudriaan, F., and Sonnemans, J. W. M., *Anal. Lett.* **4** (11), 727 (1971).
55. Aboul-Gheit, A. K., Abdou, I. K., and Mustafa, A., *Egypt. J. Chem.* **17** (5), 617 (1974).
56. Kafka, Z., Kuraš, M., Novák, J., and Vodička, L., *Fresenius' Z. Anal. Chem.* **321** (5), 475 (1985).
57. Burwell, R. L., Jr., Haller, G. L., Taylor, K. C., and Read, J. F., *in* "Advances in Catalysis" (D. D. Eley, H. Pines, and P. B. Weisz, Eds.), Vol. 20, p. 1. Academic Press, New York, 1969.
58. Laine, R. M., *Catal. Rev.-Sci. Eng.* **25** (3), 459 (1983).
59. Laine, R. M., *J. Mol. Catal.* **21,** 119 (1983).
60. Laine, R. M., *Ann. NY Acad. Sci.* **415,** 271 (1983).
61. Beuther, H., and Larson, O. A., *Ind. Eng. Chem. Process Des. Dev.* **4** (2), 177 (1965).
62. Jossens, L. W., and Petersen, E. E., *J. Catal.* **73,** 366 (1982).
63. Jossens, L. W., and Petersen, E. E., *J. Catal.* **73,** 377 (1982).
64. Satterfield, C. N., "Heterogeneous Catalysis in Practice." McGraw–Hill, New York, 1980.
65. Catry, J.-P., and Jungers, J.-C., *Bull. Soc. Chim. France,* 2317 (1964).
66. Hogan, P., and Pašek, J., *Collect. Czech. Chem. Commun.* **39,** 3696 (1974).
67. Maxwell, I. E., and van de Griend, J. A., *in* "New Developments in Zeolite Science and Technology" (Y. Murakami, *et al.,* Eds.), Studies in Surface Science and Catalysis, Vol. 28, p. 795. Kodansha, Tokyo, 1986.
68. Szépe, S., and Levenspiel, O., *in* "Proceedings, 4th European Symposium Chem. React. Eng.," p. 265. Pergamon Press, Oxford, 1971.
69. Butt, J. B., Wachter, C. K., and Billimoria, R. M., *Chem. Eng. Sci.* **33,** 1321 (1978).